AD-A123 527 THE EFFECTS OF HOT ISOSTATIC PRESSING ON MICROSTRUCTURE 1/1
AND PROPERTIES OF.. (U) PENNSYLVANIA STATE UNIV
UNIVERSITY PARK APPLIED RESEARCH LAB.. K G EWSUK
UNCLASSIFIED 30 NOV 82 ARL/PSU/TM-82-238 F/G 11/2 NL

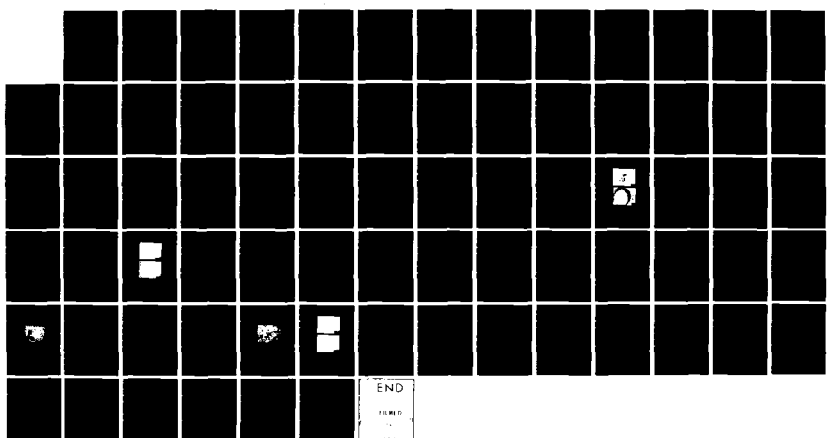

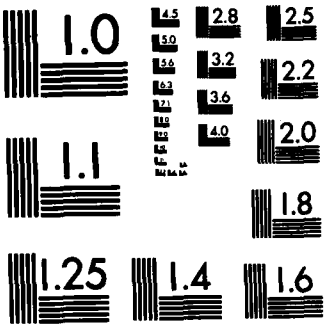

MICROCOPY RESOLUTION TEST CHART
NATIONAL BUREAU OF STANDARDS-1963-A

THE EFFECTS OF HOT ISOSTATIC PRESSING ON MICROSTRUCTURE AND PROPERTIES OF SINTERED LEAD ZIRCONATE TITANATE

Kevin G. Ewsuk

Technical Memorandum
File No. TM 82-238
November 30, 1982
Contract No. N00024-79-C-6043

Copy No. 6

The Pennsylvania State University
Intercollege Research Programs and Facilities
APPLIED RESEARCH LABORATORY
Post Office Box 30
State College, Pa. 16801

NAVY DEPARTMENT

NAVAL SEA SYSTEMS COMMAND

UNCLASSIFIED

SECURITY CLASSIFICATION OF THIS PAGE (When Data Entered)

REPORT DOCUMENTATION PAGE		READ INSTRUCTIONS BEFORE COMPLETING FORM
1. REPORT NUMBER 82-238	2. GOVT ACCESSION NO. A123 527	3. RECIPIENT'S CATALOG NUMBER
4. TITLE (and Subtitle) THE EFFECTS OF HOT ISOSTATIC PRESSING ON MICROSTRUCTURE AND PROPERTIES OF SINTERED LEAD ZIRCONATE TITANATE		5. TYPE OF REPORT & PERIOD COVERED M.S. Thesis, November 1982 6. PERFORMING ORG. REPORT NUMBER 82-238
7. AUTHOR(s) Kevin G. Ewsuk		8. CONTRACT OR GRANT NUMBER(s) N00024-79-C-6043
9. PERFORMING ORGANIZATION NAME AND ADDRESS The Pennsylvania State University Applied Research Laboratory, P.O. Box 30 State College, PA 16801		10. PROGRAM ELEMENT, PROJECT, TASK AREA & WORK UNIT NUMBERS
11. CONTROLLING OFFICE NAME AND ADDRESS Naval Sea Systems Command Department of the Navy Washington, DC 20362		12. REPORT DATE November 30, 1982 13. NUMBER OF PAGES 74 pages
14. MONITORING AGENCY NAME & ADDRESS(if different from Controlling Office)		15. SECURITY CLASS. (of this report) 15a. DECLASSIFICATION/DOWNGRADING SCHEDULE

16. DISTRIBUTION STATEMENT (of this Report)

Approved for public release, distribution unlimited,
per NSSC (Naval Sea Systems Command), January 3, 1983

17. DISTRIBUTION STATEMENT (of the abstract entered in Block 20, if different from Report)

18. SUPPLEMENTARY NOTES

19. KEY WORDS (Continue on reverse side if necessary and identify by block number)

thesis, ceramics, hot, isostatic, pressing, microstructure

20. ABSTRACT (Continue on reverse side if necessary and identify by block number)

The effects of hot isostatic pressing on the physical and electrical properties of sintered lead zirconate titanate are presented. Hot isostatic pressing for short times (<1 hour) with low applied pressures (6.9 - 20.7 MPa) at 1300°C is shown to produce lead zirconate titanate with a higher density than that obtained by conventional sintering techniques. Densification is shown to occur without an appreciable change in grain size. Localized microstructural inhomogenieties observed after pressing indicate the migration of a $PbTiO_3$-rich lead zirconate titanate liquid to pores during hot isostatic pressing. The

DD FORM 1 JAN 73 1473 EDITION OF 1 NOV 65 IS OBSOLETE

UNCLASSIFIED

SECURITY CLASSIFICATION OF THIS PAGE (When Data Entered)

rapid initial increase in density and shrinkage of macropores (>100 micrometers in diameter) indicates that rearrangement and/or solution-precipitation initially control densification during hot isostatic pressing. A decreased rate of macropore shrinkage for extended pressing times indicates that solid state diffusion controls the later stage of pore shrinkage.

For the conditions studied, hot isostatic pressing is shown to have no effect on the unclamped dielectric constant, dissipation factor, piezoelectric coefficient d_{33}, radial coupling coefficient, radial frequency constant, and Young's modulus of sintered lead zirconate titanate. However, the reduction of large voids via hot isostatic pressing improves dielectric breakdown strength.

ABSTRACT

The effects of hot isostatic pressing on the physical and electrical properties of sintered lead zirconate titanate are presented. Hot isostatic pressing for short times (<1 hour) with low applied pressures (6.9 - 20.7 MPa) at 1300°C is shown to produce lead zirconate titanate with a higher density than that obtained by conventional sintering techniques. Densification is shown to occur without an appreciable change in grain size. Localized microstructural inhomogenieties observed after pressing indicate the migration of a $PbTiO_3$-rich lead zirconate titanate liquid to pores during hot isostatic pressing. The rapid initial increase in density and shrinkage of macropores (~100 micrometers in diameter) indicates that rearrangement and/or solution-precipitation initially control densification during hot isostatic pressing. A decreased rate of macropore shrinkage for extended pressing times indicates that solid state diffusion controls the later stage of pore shrinkage.

For the conditions studied, hot isostatic pressing is shown to have no effect on the unclamped dielectric constant, dissipation factor, piezoelectric coefficient d_{33}, radial coupling coefficient, radial frequency constant, and Young's modulus of sintered lead zirconate titanate. However, the reduction of large voids via hot isostatic pressing improves dielectric breakdown strength.

TABLE OF CONTENTS

LIST OF TABLES

LIST OF TABLES (continued)

LIST OF FIGURES

LIST OF FIGURES (continued)

ACKNOWLEDGMENTS

The author expresses his appreciation to Dr. Milivoj Brun for conducting high pressure hot isostatic pressing experiments, and to Dr. Walter S. Schulze for his consultation on lead zirconate titanate ceramics. The time and efforts of all others who assisted in this study are also greatly appreciated. Special thanks go to Dr. Gary L. Messing for his advice and consultation throughout this study.

This study was funded by The Pennsylvania State University Applied Research Laboratory under contract with the U.S. Naval Sea Systems Command.

INTRODUCTION AND STATEMENT OF THE PROBLEM

The deleterious effects of porosity in ceramic bodies are well demonstrated throughout the literature. Porosity is especially troublesome in ferroelectric ceramics as increased amounts of porosity severely degrade electrical properties, and large voids can result in dielectric breakdown during poling or in service. These adverse effects can be avoided if the proper processing technique(s) is used to produce a dense homogeneous microstructure. One technique that is proposed to increase density and improve microstructure in sintered bodies is hot isostatic pressing.

This study will focus on hot isostatic pressing sintered lead zirconate titanate, a common ferroelectric ceramic, with the objectives of:

1. determining if hot isostatic pressing is a viable means of densifying sintered lead zirconate titanate;
2. determining the mechanism(s) by which lead zirconate titanate densifies during hot isostatic pressing; and
3. determining if hot isostatic pressing is a viable means of improving the electrical properties of sintered lead zirconate titanate.

LITERATURE REVIEW

Lead Zirconate Titanate

Lead zirconate titanate,[1] which will be referred to as PZT throughout this thesis, represents a series of solid solutions of lead zirconate ($PbZrO_3$) and lead titanate ($PbTiO_3$) in which Zr^{+4} and Ti^{+4} occupy like positions in a perovskite-type structure (Figure 1). As demonstrated in Figure 2, the $PbZrO_3$-$PbTiO_3$ system exhibits complete solid solubility and is comprised of a number of different phases. The useful forms of PZT are found at the lower temperatures (<500°C) as they display ferroelectric and subsequently piezoelectric behavior.

Lead zirconate titanate has the ability to transform energy between the electrical and mechanical forms, making it a useful material for electromechanical transducer devices such as phonographic pickups, air and underwater (sonar) transducers, accelerometers, and high-voltage generators. In recent times it has become the foremost material used in the production of these devices.

The dominance of PZT in the electromechanical transducer industry can be attributed to the superior piezoelectric properties of PZT and the ability to manipulate these properties to meet the specific requirements for the above applications. The piezoelectric and electromechanical coupling coefficients of PZT are among the best known, and persist over a wide range of temperatures. Furthermore, these properties and others, such as dielectric constant, dielectric loss, and mechanical quality factor, can be adjusted by

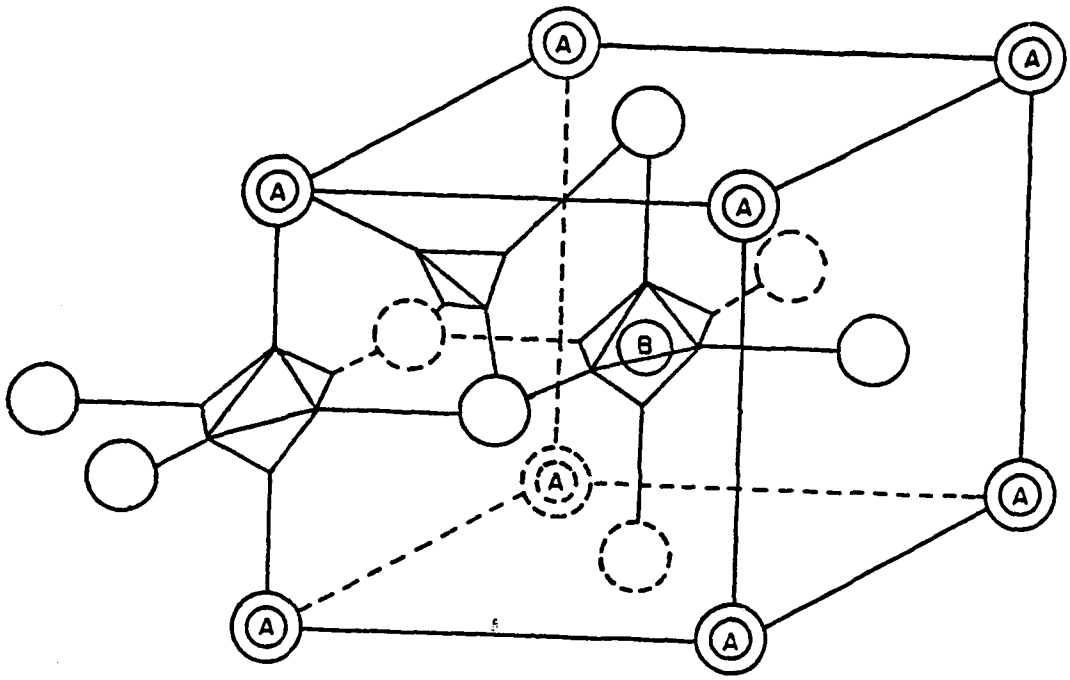

Figure 1. Diagram of the perovskite unit cell. Open circles are oxygen; A and B cation sites are occupied by Pb and (Zr,Ti), respectively.[1]

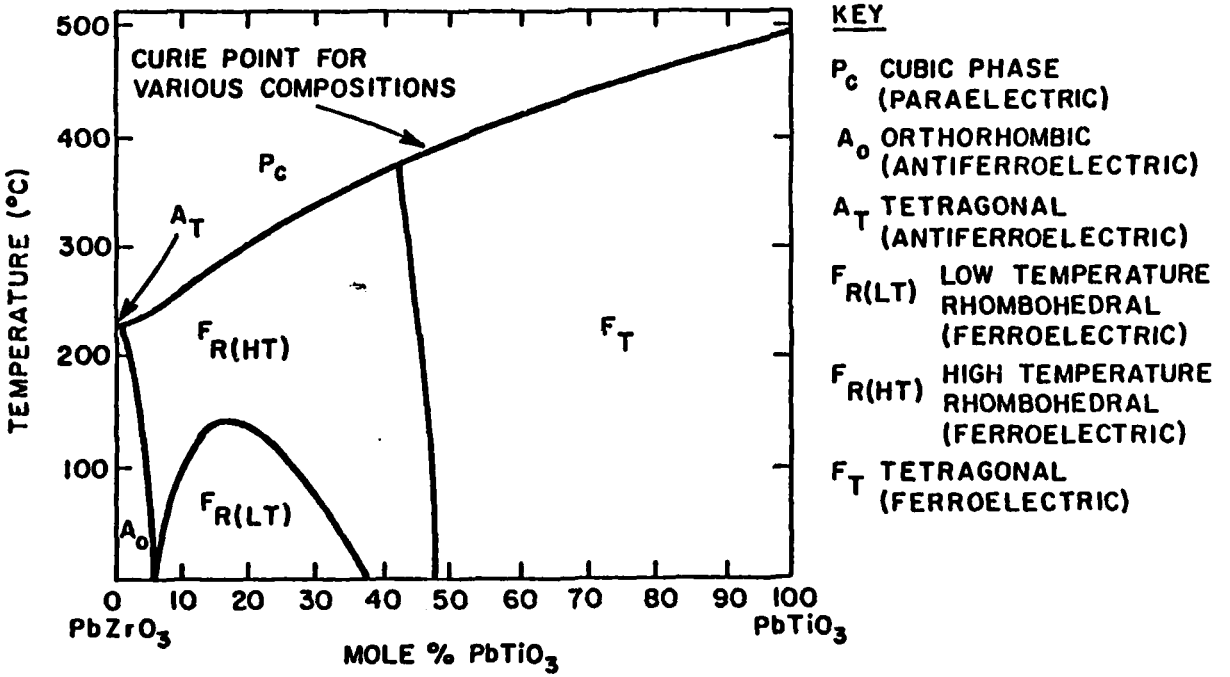

Figure 2. The sub-solidus $PbZrO_3$-$PbTiO_3$ phase diagram.[1]

varying composition. The solid solubility in the PZT system affords it the flexibility to easily vary composition via changes in the $PbZrO_3$:$PbTiO_3$ molar ratio. Additionally, properties can be modified with dopants such as Sr, Nb, and Bi.[3-9]

An example of a commercial PZT that has been chemically adjusted for a particular application is $Pb_{0.94}Sr_{0.06}Zr_{0.53}Ti_{0.47}O_3$. This material, which was exclusively used in this study, is suitable for the production of electromechanical drivers (e.g., ultrasonic mixers). By partially substituting Sr^{+2} for Pb^{+2}, the electromechanical coupling coefficients, piezoelectric constants, and dielectric constant all show improvements over the values for undoped PZT. Also, dielectric losses remain low, ensuring an efficient conversion of energy without the production of excessive amounts of heat. Furthermore, the Sr^{+2} addition increases the ability of the PZT to withstand the large electrical or mechanical forces an electromechanical driver is subjected to without depoling. The 0.53:0.47 $PbZrO_3$:$PbTiO_3$ molar ratio is used to maximize the dielectric properties. As demonstrated in Figure 3, the highest dielectric constants and radial coupling coefficients are exhibited near the rhombohedral-tetragonal morphotropic boundary (~53 mole % $PbZrO_3$, 47 mole % $PbTiO_3$ at 25°C) and thus this is the favored composition range for commercial applications.

Although modification of the chemical composition permits a great deal of flexibility in property design, it is also one of the major reasons for the difficulty in manufacturing PZT with reproducible properties.[10-14] The properties of PZT are quite sensitive to chemical and physical variations and, as shown in a

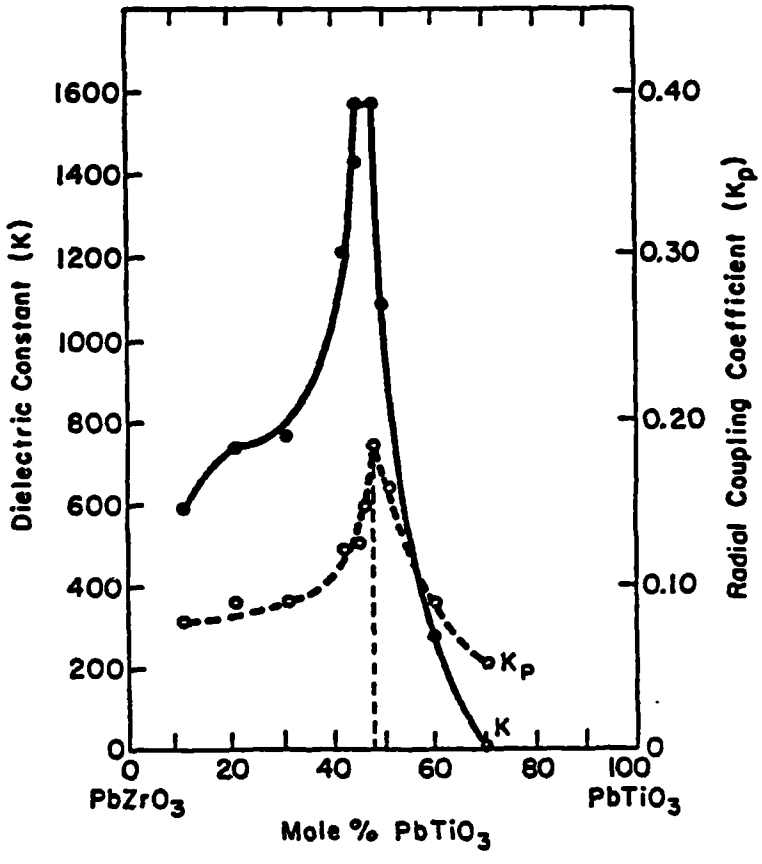

Figure 3. Dielectric constant and radial coupling coefficient as a function of composition in the $PbZrO_3$-$PbTiO_3$ system at 25°C.[1]

recent study,[2] the inability to maintain chemistry in a narrow composition range during processing and to avoid fluctuations in raw material properties (e.g., grain size) can lead to significant variations from lot to lot.

Powder Synthesis

The synthesis of PZT plays an important role in reproducibly obtaining good properties. While good quality PZT can be consistently produced by co-precipitation[15-17] and sol-gel[18] methods, these techniques are too involved and costly for most commercial operations. Therefore, manufacturers rely on the somewhat less consistent method of calcining $PbCO_3$, ZrO_2, and TiO_2.[2,19,20] Studies[2,20] have shown that for this method, inconsistencies in raw material sources, dispersion of the raw materials, and calcining procedure can result in the production of powders with differences significant enough to alter the properties obtained in sintered bodies.

Sintering

The volatility of PbO at high temperatures makes sintering a critical step in producing high-quality PZT ceramics as volatilization will alter both stoichiometry and the densification process. Kingon[2] demonstrated that PbO volatilization could be prevented by controlling the activity of PbO vapor in the sintering atmosphere. He studied three different ways to control PbO activity, including the addition of excess PbO to the PZT powder, burying pieces in a PbO "source" powder during sintering, and sintering pieces in the presence of, but

not in contact with, a source powder. His investigations showed that volatilization could adequately be controlled by both the second and third methods with the best results obtained from the latter.

In addition to stoichiometry, microstructure must also be controlled during sintering as it too will significantly affect final properties. Porosity, especially, has been shown to have an adverse effect on electrical properties, particularly dielectric breakdown.[21,22] It has also been demonstrated that properties are dependent on grain size,[23] although to a lesser degree. Since excessive grain growth is not usually observed in PZT, the objective of sintering is to produce high-density bodies while maintaining stoichiometry.

Even though a number of sintering studies have been conducted on PZT,[2,9,10,16,19,24-32] the exact mechanisms of densification have yet to be determined. This may be due to the complex nature in which PZT densifies as well as indications that different mechanisms may be dominant in different systems. High densities can be obtained with most commercial PZT by sintering at approximately 1300°C. The high temperature phase diagram for the $PbZrO_3$-$PbTiO_3$ system (Figure 4) indicates that densification should then occur by a solid state diffusion process. However, common dopants such as Bi and Sr are believed to act as fluxes in this system, creating thin films of liquid between grains that allow densification to proceed by a liquid phase sintering mechanism.[7,28,29] Atkin and Fulrath[24] have suggested that the rate-limiting step for densification in any PZT is the diffusion of oxygen vacancies from pores to grain boundaries

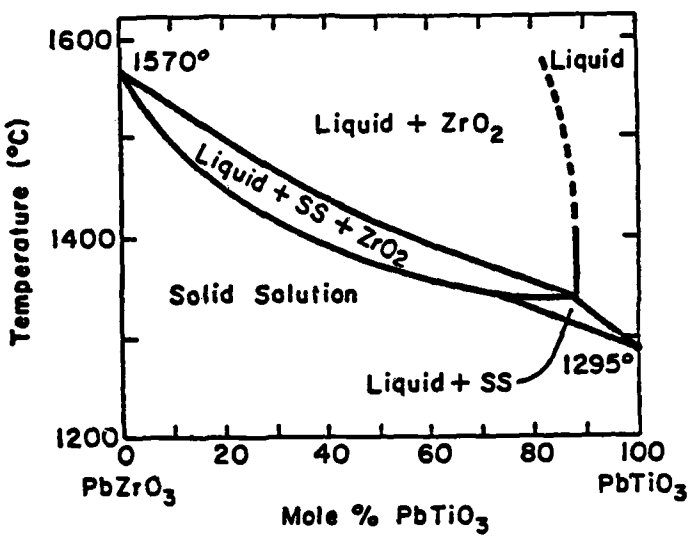

Figure 4. The high temperature $PbZrO_3$-$PbTiO_3$ phase diagram.[1]

where they are annihilated. Results from a recent study by Kingon[2] are in accordance with this postulate.

The density obtained by sintering PZT usually varies from 95 to 97% of the theoretical value. To maximize electrical properties and ensure their reproducibility, attempts have been made to improve upon this. Additions of silica[10] and alumina[28] have been shown to create a low melting second phase in PZT that enhances densification by a liquid phase sintering process. However, these additions also have adverse effects on electrical properties. More successful ways of producing dense, good-quality PZT ceramics have been by sintering in oxygen,[31,32] hot pressing, and hot isostatic pressing.

Hot Pressing

Hot pressing is a specialized processing method used to obtain high densities in sintered bodies. Its advantage over conventional sintering is that in addition to using elevated temperatures to densify a piece, uniaxial pressure is also applied on the body. The pressure increases the driving force for densification, making it possible to obtain higher densities.[33-37]

Hot pressing has proven to be a viable means of producing high-density PZT ceramics.[11,14,38-41] Since densification can occur at lower temperatures and in shorter times, PbO volatilization is suppressed and thus stoichiometry remains relatively unchanged during processing.[14,38] Consequently, hot pressing can produce properties superior to those obtained by conventional sintering.

Balkevich and Flidlider[39] extensively studied the hot pressing

of PZT with emphasis on determining the densification mechanisms associated with this process. They observed a very rapid rate of densification initially, which slowed considerably in the intermediate stage and was negligible in the end. From these and other observations, they concluded that densification occurred by rearrangement in the initial stage, plastic deformation in the intermediate stage, and diffusional creep in the final stage of densification. Additionally, they showed that the use of excessive pressures could produce grain cracking and deformation that adversely affect electrical properties, including a reduction of the dielectric constant and a weakening of the piezoeffect.

Hot Isostatic Pressing

Hot isostatic pressing[42-48] or HIP, as it is referred to in this thesis, is the simultaneous application of elevated temperature and isostatic pressure to an object via an inert gas phase (e.g., argon). Like hot pressing, it has an increased driving force for densification that allows it to produce high-density bodies with lower processing temperatures and shorter times. However, since pressure is applied isostatically, it has additional advantages that hot pressing does not. A distinct advantage is that HIPing has virtually no shape limitations, so pieces can be sized and shaped prior to firing, avoiding the excessive costs of machining later. Also, texture is not induced with isostatic pressure so idealized microstructures with good homogeniety are produced. Furthermore, since pressure is applied via a gas phase, there is no need for dies, so problems with die contamination and die life are avoided.

One requirement of this process is that, in order to transmit the pressure to the rest of the body, the surface of the object being HIPed must be impermeable to the pressurizing gas. This is not a difficult prerequisite to meet since impermeable surfaces are easily produced by hermetically sealing pieces in glass or metal canisters or sintering the piece to the closed porosity state (>92% theoretical density) prior to HIPing.

A number of studies have been conducted on the HIPing of PZT[49-54] with overall indications that a more uniform, high-density, high-quality electroceramic is produced. The most explicit study to date was conducted by Bowen et al.[49] They showed that lower dielectric losses and substantially improved dielectric breakdown strengths could be obtained by HIPing. Although their study did not concentrate on determining the densification mechanisms associated with HIP, it was suggested that, as in hot pressing, densification occurs by a combination of rearrangement, plastic flow, and diffusional creep. It was also postulated that densification may simultaneously be occuring by the extrusion of a liquid phase into the pores.

EXPERIMENTAL PROCEDURE

Powder Preparation and Characterization

A commercial lead zirconate titanate powder, UPI 401,[a] was used exclusively throughout this study. To enhance the sintering reactivity of the powder, the coarse fraction (≥6 micrometers) of its particle size distribution was removed with an Acucut air classifier.[b] The particle size was then determined by sedimentation with a Sedigraph 5000.[c] The chemical composition of the powder was determined by both emission spectroscopy[d] and x-ray diffraction with CuK_α radiation. For the latter, peak positions generated in the 43-48° 2θ range were compared to those obtained from standards to accurately determine the molar ratio of $PbZrO_3$:$PbTiO_3$.[2]

Sample Preparation

To prepare the PZT for pressing, two volume percent of an acrylic wax emulsion (Rhoplex B-60A)[e] was added to the beneficiated powder. A homogeneous dispersion was ensured by first forming a slurry. The slurry was then dried and screened through a 200-mesh (105 micrometer) sieve. In order to have a reference for monitoring

---

[a] Ultrasonic Powders, Inc., South Plainfield, NJ 07080.

[b] Donaldson Co., Inc., Minneapolis, MN 55440.

[c] Micromeretics Instrument Corp., Norcross, GA 30071.

[d] Mineral Constitution Lab, The Pennsylvania State University, University Park, PA 16802.

[e] Rohm and Haas, Philadelphia, PA 19105.

microstructural changes during the HIP experiments, pores of a distinct size and geometry were introduced into the sintered body by adding 100 ± 5 micrometer polymethyl methacrylate spheres[f] to the green powder. Samples were prepared by hand mixing 0.0025 g (~5000 in number) of the spheres into 3 g of the powder-binder mixture. To reduce preferential pressing defects, pellets were formed by first uniaxially pressing them at 30 MPa in a 1.27 cm diameter stainless steel die, then isostatically pressing them at 172 MPa. All of the organics were burned out of the pellets by heating to 500°C at 10°C/minute and holding for one hour. To determine the effects of HIP on samples lacking gross porosity, pellets were also formed without the macropore addition. Densities of the green pellets were determined by dimension.

Sintering

For the hot isostatic pressing experiments, it was required to have closed porosity in the samples. This was obtained by sintering the pellets at 1320°C for one hour in an O_2 atmosphere. Oxygen was used to avoid entrapping a gaseous species (i.e., N_2) in the pore phase that would not readily diffuse through the sample during HIPing. To prevent excessive lead oxide volatilization during sintering, the pellets were packed in a combination of sintered and green PZT powders and enclosed in a platinum-lined alumina crucible (Figure 5). Densities of the sintered pellets were determined by Archimedes' method.

---

[f]Polysciences, Inc., Warrington, PA 18976.

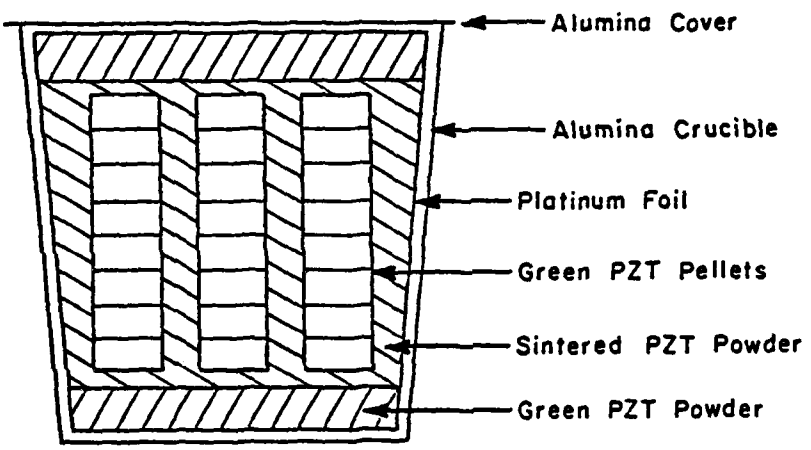

Figure 5. The configuration of PZT pellets and packing powders used to prevent excessive lead oxide volatilization during sintering.

Hot Isostatic Pressing

The sintered samples were HIPed at 1300°C with argon gas. To prevent lead oxide volatilization during HIPing, the pellets were enclosed in a platinum-lined alumina crucible along with a green PZT pellet as a lead oxide source (Figure 6). Due to equipment limitations, this study concentrated on using relatively low applied pressures (6.9, 13.8, and 20.7 MPa) to densify the pellets. To study densification kinetics, HIP times were varied from 7.5 to 60 minutes. The effect of higher pressures (69, 138, and 207 MPa for 15 minutes) was also investigated.[g] However, an accurate assessment of the results could not be made as the samples were severely reduced in the graphite furnace. Therefore, these experiments were terminated. With the exception of the high pressure experiments, all HIPing was completed in the autoclave illustrated in Figure 7. A typical HIP run involved first heating the samples to 1300°C, applying the pressure for the requisite time, then rapidly reducing both temperature and pressure (Figure 8). Densities of the HIPed pellets were determined by Archimedes' method.

Compositional Analysis

To determine if any significant changes in gross stoichiometry occurred during processing, the chemical composition of sintered and HIPed pellets was determined by emission spectroscopy and x-ray

---

[g]General Electric Corporate Research and Development, Schenectady, NY 12019.

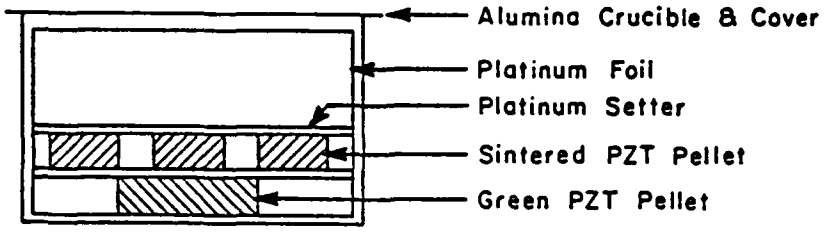

Figure 6. The configuration of sintered and green source pellets used to prevent lead oxide volatilization during HIPing.

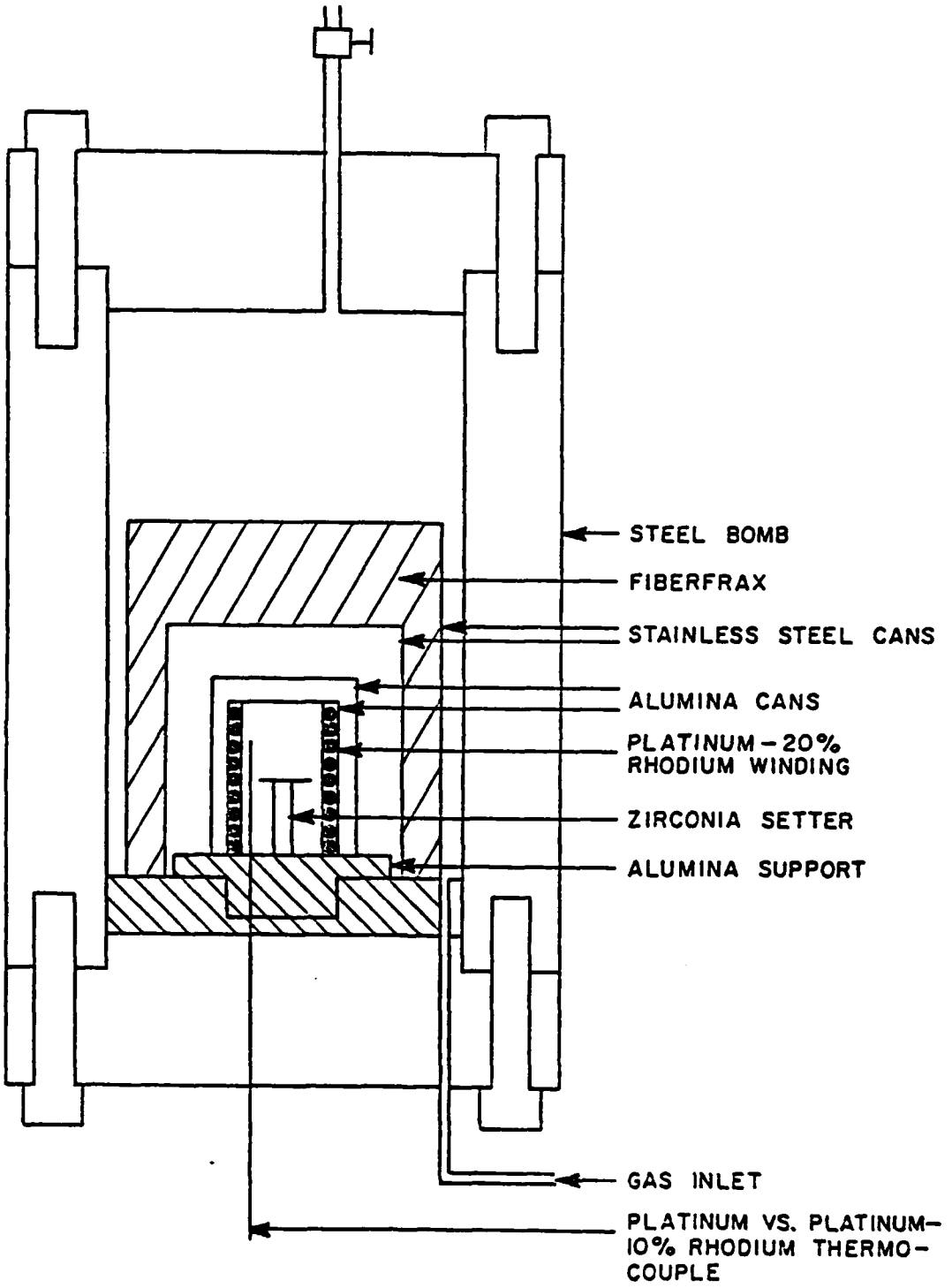

Figure 7. The hot isostatic press used for low pressure experiments.

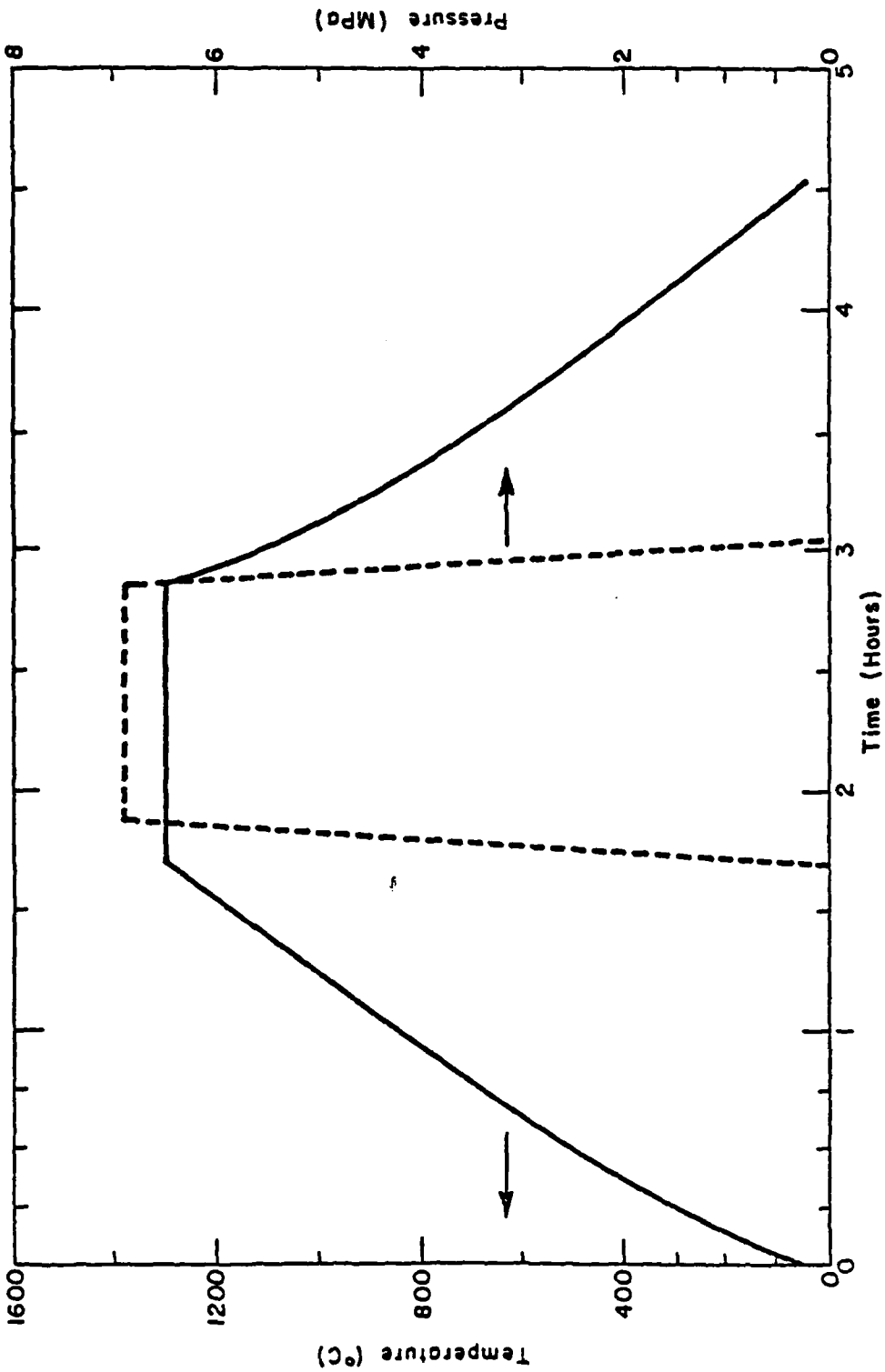

Figure 8. A typical pressure-temperature cycle used in the HIP studies. The solid line represents the temperature curve while the broken line represents the pressure curve.

diffraction. Energy dispersive spectroscopy (EDS)[h] on a scanning electron microscope (SEM)[i] was used to identify localized compositional variations in the sintered and HIPed pellets. These variations were then quantified by electron microprobe analysis[j] with reference to standards.

Microstructural Analysis

Microstructures of sintered and HIPed pellets were studied on the SEM. The two features of interest were macroporosity and grain size. To reveal both macrovoids and grain size, samples were prepared by cutting the pellets in half, polishing with 0.25 micrometer diamond paste, and etching with a solution of 70 v/o H_2O - 29.5 v/o HNO_3 - 0.5 v/o HF at 80°C for 40 seconds. Macropore size was measured directly from the SEM image while grain size was determined from SEM photographs of randomly selected regions. In both cases, it was assumed that uniform size and equiaxed geometries were being measured so that the average size of macropores and grains could be calculated by applying the appropriate correction factor of 1.5 times the measured average linear intercept.[55]

Electrical Property Measurements

To determine if HIPing had any significant effect on electrical

---

[h] Kevex Corp., Foster City, CA 94404.

[i] International Scientific Instruments, Inc., Santa Clara, CA 95051.

[j] Perkin-Elmer ETEC, Inc., Hayward, CA 94544.

properties,* the capacitance, dissipation factor, piezoelectric coefficient d_{33}, and radial coupling coefficient of ~10.4 mm in diameter by ~0.06 mm thick sintered and HIPed samples were measured. In preparation for these measurements, the samples were first electroded. To ensure the formation of good electrical contacts, sputtered gold electrodes with a protective coating of silver paint were used. To avoid property variations resulting from residual strains produced by variable cooling rates, all samples were heated above the Curie temperature to 400°C, held for 10 minutes, and slowly cooled to room temperature. The PZT samples were poled by placing them in an oil bath at 145°C for 15 minutes while an electrical potential of 22.5 kV/cm was applied across its thickness. To avoid the unstable properties apparent immediately following poling, the samples were aged 48 hours before taking any measurements. Capacitance and dissipation factor were measured at frequencies varying from 100 Hz to 4 MHz on a Hewlett-Packard multi-frequency LCR meter.[k] The relative free dielectric constant at 1000 Hz was determined from these measurements. The piezoelectric coefficient d_{33} was measured at 100 Hz on a Berlincourt piezo d_{33} meter.[1] The radial coupling coefficient was determined by the resonance method described in the IRE standards.[56] The resonance measurements, which were made on a Hewlett-Packard 3585A spectrum analyzer,[k] were also used to determine Young's modulus Y_{11} and radial frequency constant.

---

[k]Hewlett-Packard Company, Palo Alto, CA 94304.

[1]Channel Products, Inc., Chagrin Falls, OH 44022.

*A basic understanding of the electrical terms used is assumed. For additional information on them, the reader is referred to Jaffe et al.[1]

RESULTS AND DISCUSSION

Powder Characteristics

As previously stated, the commercial PZT powder designated as 401 by the manufacturer was used exclusively throughout this study. After air classification the particle size distribution of the powder showed a median particle size of 2.3 micrometers with 90% of the distribution between 1 and 4 micrometers (Figure 9).

Composition and Structure

From emission spectroscopy the chemical composition of the powder was determined to be $Pb_{0.94}Sr_{0.06}Zr_{0.50}Ti_{0.50}O_3$. It is important to note that neither sintering at 1320°C for 1 hour nor HIPing at 1300°C for up to 2 hours with pressures of 6.9 to 20.7 MPa resulted in significant changes in composition (Table 1). This is consistent with the weight loss measurements used to monitor PbO volatilization which showed that sintered samples experienced only 0.3% weight loss and HIPed samples experienced none.

From x-ray diffraction analysis, it was determined that the structure of the PZT is tetragonal. Comparing the diffraction peaks obtained from this powder to those from standards, the $PbZrO_3$:$PbTiO_3$ molar ratio was determined to be 0.53:0.47. This ratio is not in agreement with that obtained by emission spectroscopy. However, by comparing the diffraction patterns for green, sintered, and HIPed PZT (Figure 10), it can be seen that peak positions are identical.

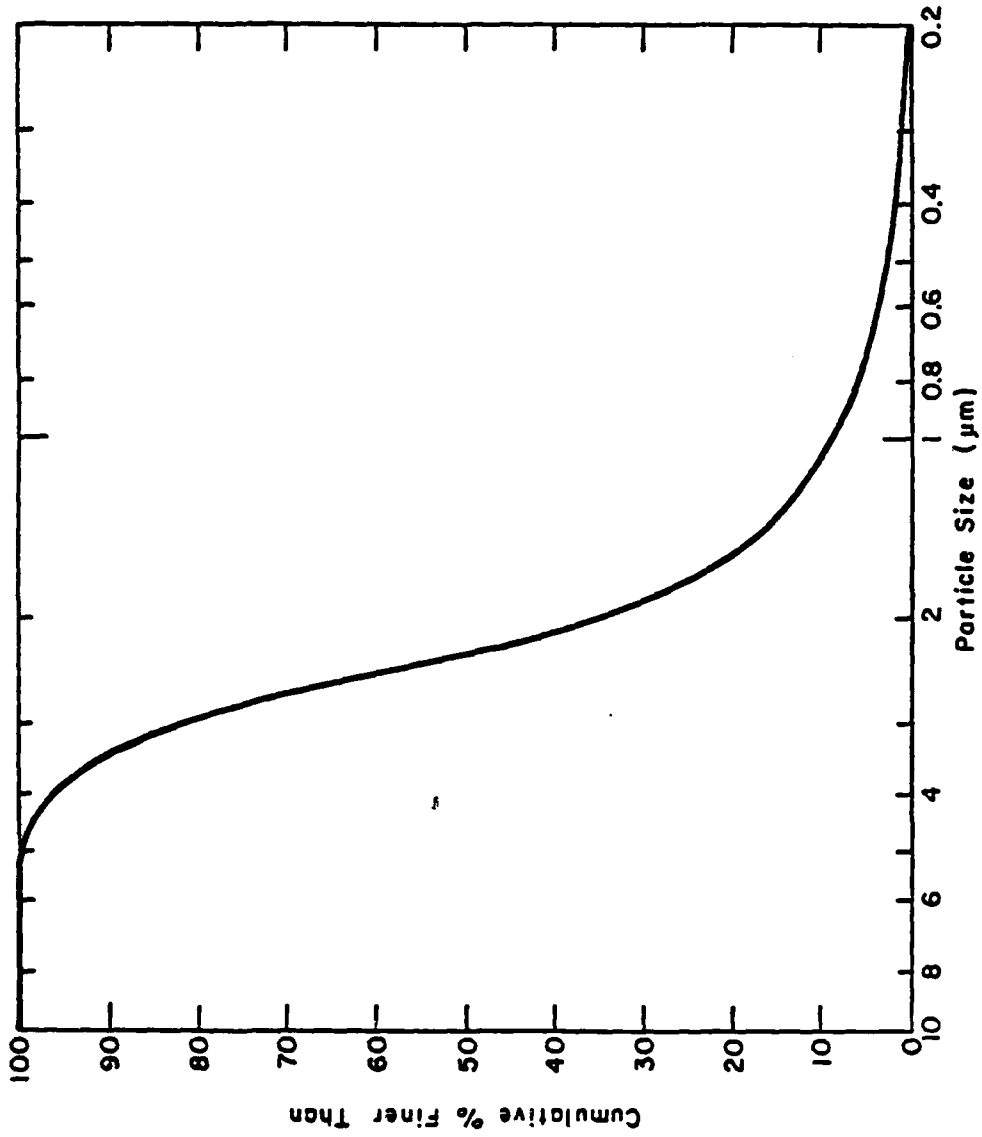

Figure 9. Particle size distribution of the PZT powder.

Table 1

Emission Spectrographic Analyses of As Received PZT, PZT After Sintering (1320°C/1 hour), and PZT After HIPing (1300°C/2 hours at 20.7 MPa)

	As Received	Sintered	HIPed
PbO (wt %)	66.1	66.0	66.0
SrO (wt %)	2.1	2.2	2.1
ZrO_2 (wt %)	19.2	19.3	19.2
TiO_2 (wt %)	12.6	12.5	12.7

This indicates that, as was observed in the emission spectroscopic analysis, composition remains essentially unchanged throughout processing. This suggests that there is a certain degree of inaccuracy associated with one of these techniques. Since the compositional analysis as determined by peak positions in x-ray diffraction patterns is well documented, it is believed that the inaccuracy is in the emission spectroscopic analysis. Thus, the composition of the PZT was approximated to be $Pb_{0.94}Sr_{0.06}Zr_{0.53}Ti_{0.47}O_3$.

Although peak positions are unchanged throughout processing, one observable difference is that the green PZT powder has broader diffraction peaks than either the sintered or HIPed PZT specimens. This may be due to the coexistence of $PbZrO_3$-rich rhombohedral PZT with $PbTiO_3$-rich tetragonal PZT in the green powder. For such a case, many peaks would be present in a narrow range of 2θ, and this would appear as a single broad peak in the diffraction pattern. Monophase PZT has distinct, sharp peaks. Kingon[2] indicated that high temperatures (>900°C) are required to produce a monophase PZT.

a)

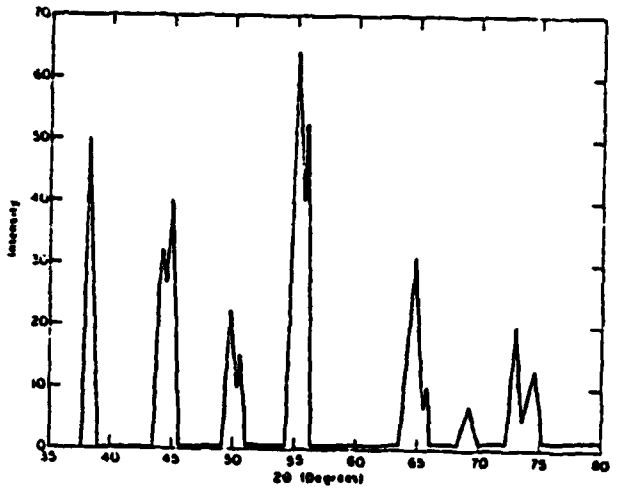

b)

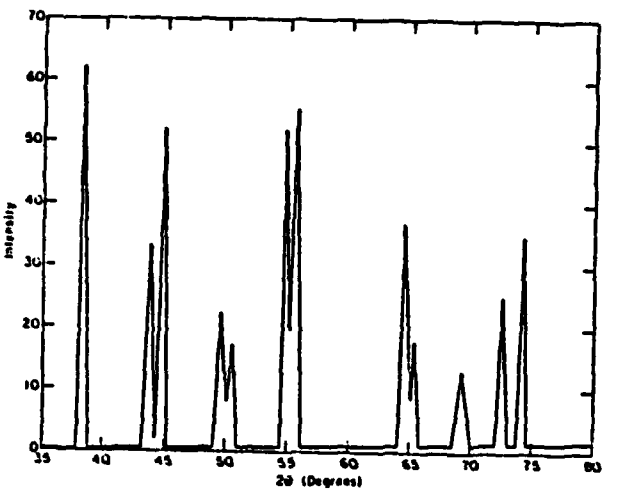

c)

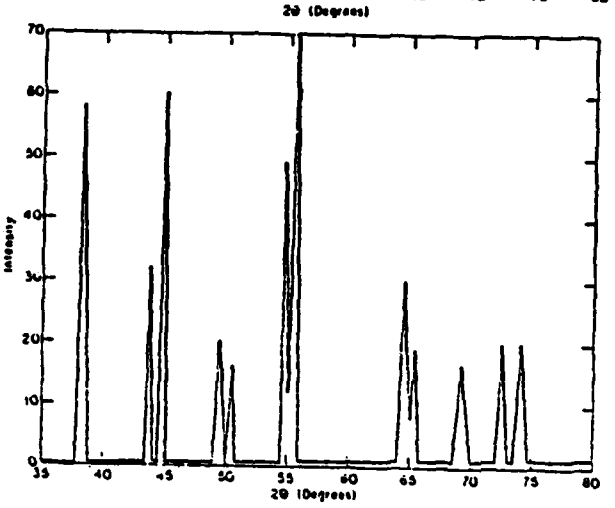

Figure 10. X-ray analyses of PZT a) green, b) sintered for 1 hour at 1320°C, and c) sintered for 1 hour at 1320°C and HIPed for 2 hours at 1300°C and 20.7 MPa.

In accordance with this, the results from this study indicate that the reaction to produce monophase tetragonal PZT occurs during sintering as the diffraction patterns for sintered and HIPed PZT are comprised of distinct, sharp peaks and are virtually identical.

Although observable variations in peak intensities exist in the diffraction patterns for the green, sintered, and HIPed PZT, it is believed that these variations are the result of orientation effects. Therefore, they are not considered pertinent to the analysis of these results. Overall, the results indicate that no major differences in composition or structure exist between sintered and HIPed PZT.

From the x-ray peak positions and the chemical composition determined above, the theoretical density of the sintered PZT was determined to be 8.00 g/cc.

Sintering

An average density of 97.3% of theoretical was obtained for all samples sintered, including both those with and without macropores added. This result indicates that the addition of polymethyl methacrylate spheres to the green body does not affect the total porosity level obtained during sintering. The size of macropores was 100 micrometers in the pellets after burnout and 123 micrometers after sintering. This indicates that the macropores grew during sintering, a common phenomenon reported in the literature.[57] The sphericity of the macropores and the surrounding dense microstructure is clearly shown in Figure 11a. At higher magnification,

a)

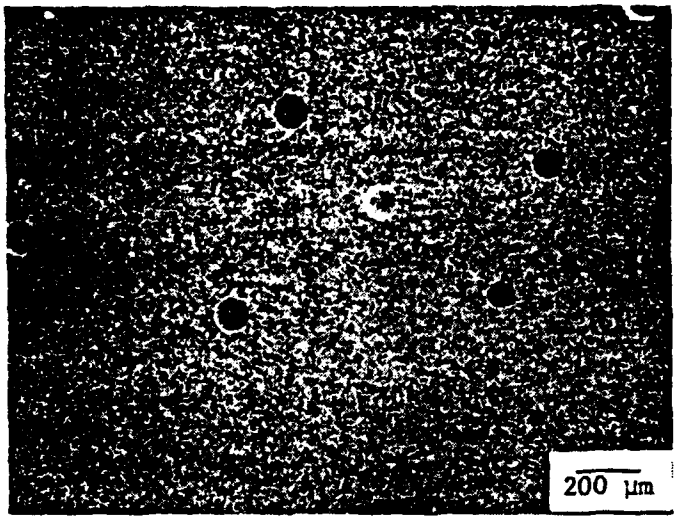

b)

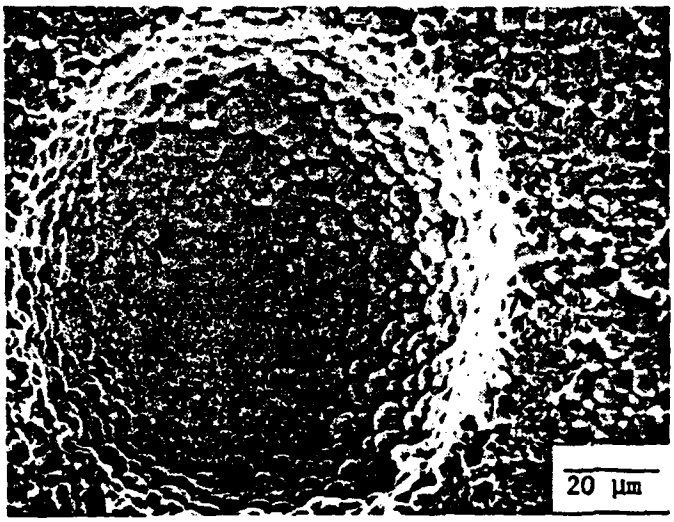

Figure 11. Photomicrograph of macroporosity in sintered PZT at a) 45x and b) 650x.

the grains at the pore surface are seen to be equiaxed with smooth surfaces (Figure 11b).

Hot Isostatic Pressing

Physical Properties. Densities after sintering at 1320°C for 1 hour and after HIPing at 1300°C and 20.7 MPa as a function of time for PZT processed without the addition of macropores are presented in Table 2. Based on the accuracy of the Archimedes' technique, the values reported are accurate to ±0.1%. Only the high pressure (20.7 MPa) HIP results are presented as the greatest change in density would be expected for these experiments. In general, it is evident that HIPing at these presures slightly improves the density of sintered PZT.

Table 2

Density of PZT Without Macropores After Sintering for 1 Hour at 1320°C, and After HIPing as a Function of Time at 1300°C and 20.7 MPa

HIP Time (min)	Sintered Density (%)	HIPed Density (%)
0.0	97.32	97.32
7.5	97.10	97.67
15.0	97.80	97.87
30.0	97.70	97.82
60.0	96.10	97.80

The changes in the physical properties of PZT (with macropores added) as a function of HIP time at 1300°C and pressures of 6.9,

13.8, and 20.7 MPa are reported in Tables 3-5, respectively. Based on the accuracy of the average linear intercept technique, the grain and macropore sizes reported are accurate to ±0.01%. The results show the trends apparent for each set of parameters studied, with similar trends observed for all three pressing pressures.

In general, HIPing results in a slight increase in density, with the majority of densification occurring in short times (≤ 15 minutes). At longer HIP times the densities remain relatively unchanged. This suggests that a two-stage densification process with a limiting density of less than 98% of theoretical exists for these HIP conditions.

From microstructural analysis it is observed that there was no appreciable change in grain size during HIPing. As shown in Figure 12, the only observable difference between the microstructures of sintered and HIPed PZT is the presence of a "liquid phase" at triple points in the latter. Although this liquid phase is not observed in the sintered PZT, Goo et al.[58] have determined that thin films (~10nm) of a liquid phase with a high solubility of solid PZT exist between grains when excess PbO is present in the system. They also suggested that this grain boundary phase should not be very transient during sintering. This could explain why the liquid phase is not observed at triple points in the sintered PZT. It is believed that, during HIPing, the external pressure compresses the system, decreasing interparticle distances and forcing the liquid into previously porous regions. Such a mechanism has been postulated by Bowen et al.[49] Further evidence for such a process can be inferred from a discussion of liquid phase sintering by Lange.[59] He demonstrated that the amount of liquid between grains continuously decreases with

Table 3

The Physical Properties of PZT
HIPed at 1300°C and 6.9 MPa
as a Function of Time

HIP Time (min)	Sintered Density (%)	HIPed Density (%)	Average Grain Size (μm)	Average Macropore Diameter (μm)	Volume % Reduction of Macroporosity
0.0	97.32	97.32	9	123	0.0
7.5	96.49	97.48	10	96	52.2
15.0	97.03	97.59	8	103	41.3
30.0	97.15	97.64	10	96	52.5
45.0	97.55	97.73	8	96	52.5
60.0	97.15	97.62	7	95	53.9

Table 4

The Physical Properties of PZT
HIPed at 1300°C and 13.8 MPa
as a Function of Time

HIP Time (min)	Sintered Density (%)	HIPed Density (%)	Average Grain Size (μm)	Average Macropore Diameter (μm)	Volume % Reduction of Macroporosity
0.0	97.32	97.32	9	123	0.0
7.5	97.06	97.59	8	96	52.5
15.0	97.37	97.65	10	102	43.0
30.0	97.36	97.71	10	102	43.0
45.0	96.91	97.64	7	96	52.5
60.0	97.41	97.56	8	96	52.5

Table 5

The Physical Properties of PZT
HIPed at 1300°C and 20.7 MPa
as a Function of Time

HIP Time (min)	Sintered Density (%)	HIPed Density (%)	Average Grain Size (μm)	Average Macropore Diameter (μm)	Volume % Reduction of Macroporosity
0.0	97.32	97.32	9	123	0.0
7.5	97.63	98.05	8	100	46.3
15.0	97.07	97.66	8	98	49.4
30.0	96.90	97.63	10	90	60.8
45.0	97.34	97.74	9	88	63.4
60.0	97.80	97.92	9	85	67.0

a)

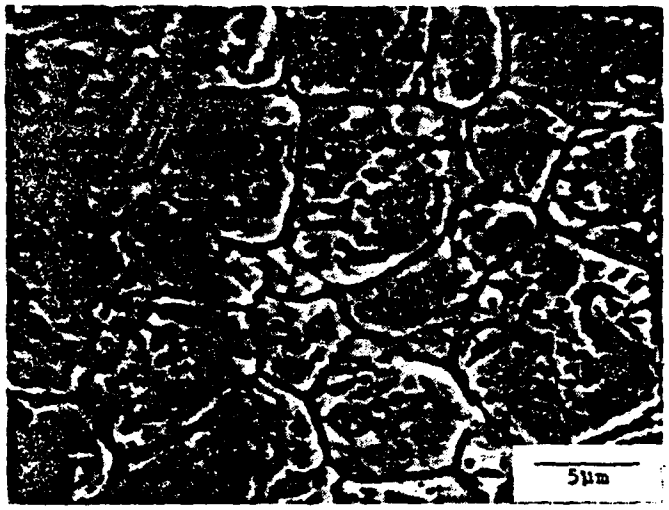

b)

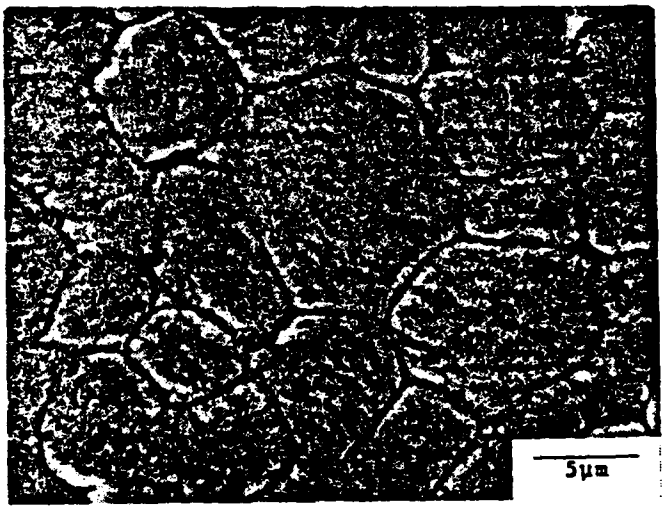

Figure 12. Photomicrograph of the microstructure of a) sintered PZT and b) PZT HIPed for 1 hour at 1300°C and 20.7 MPa.

sintering time, his calculations based on the compressive forces arising from capillary action. During HIPing, it is believed that the greater compressive forces generated by the external applied pressure enhance the rate at which this process occurs. The result is an observable migration of the liquid to previously porous regions.

It is also shown in Tables 3-5 that HIPing reduced the size of macroporosity, with large decreases observed for short times and little or no additional changes for longer times. The percent change in the volume of macroporosity ($\%\Delta V_{macro}$) as a function of HIP time was determined from the equation:

$$\%\Delta V_{macro} = \frac{D_S^3 - D_H^3}{D_S^3} \times 100$$

where D_S is the average diameter of macropores in the sintered PZT, and D_H is the average diameter of macropores in the HIPed PZT. The kinetics of the shrinkage of macroporosity are shown in Figures 13-15. It is observed that HIPing results in large volume percent reductions of the macroporosity, with the trends for this reduction the same as those observed for density changes.

To determine if macropores are preferentially reduced near the surface of the pellets during HIPing, the average size of pores near the pellet's surface was compared to that of those in the center. Since no difference was observed, it is believed that preferential densification is not a problem in HIPing PZT, at least not for the sample sizes studied.

Porosity. In addition to total and macroporosity, it was desired to see how the microporosity changed with HIP time. The

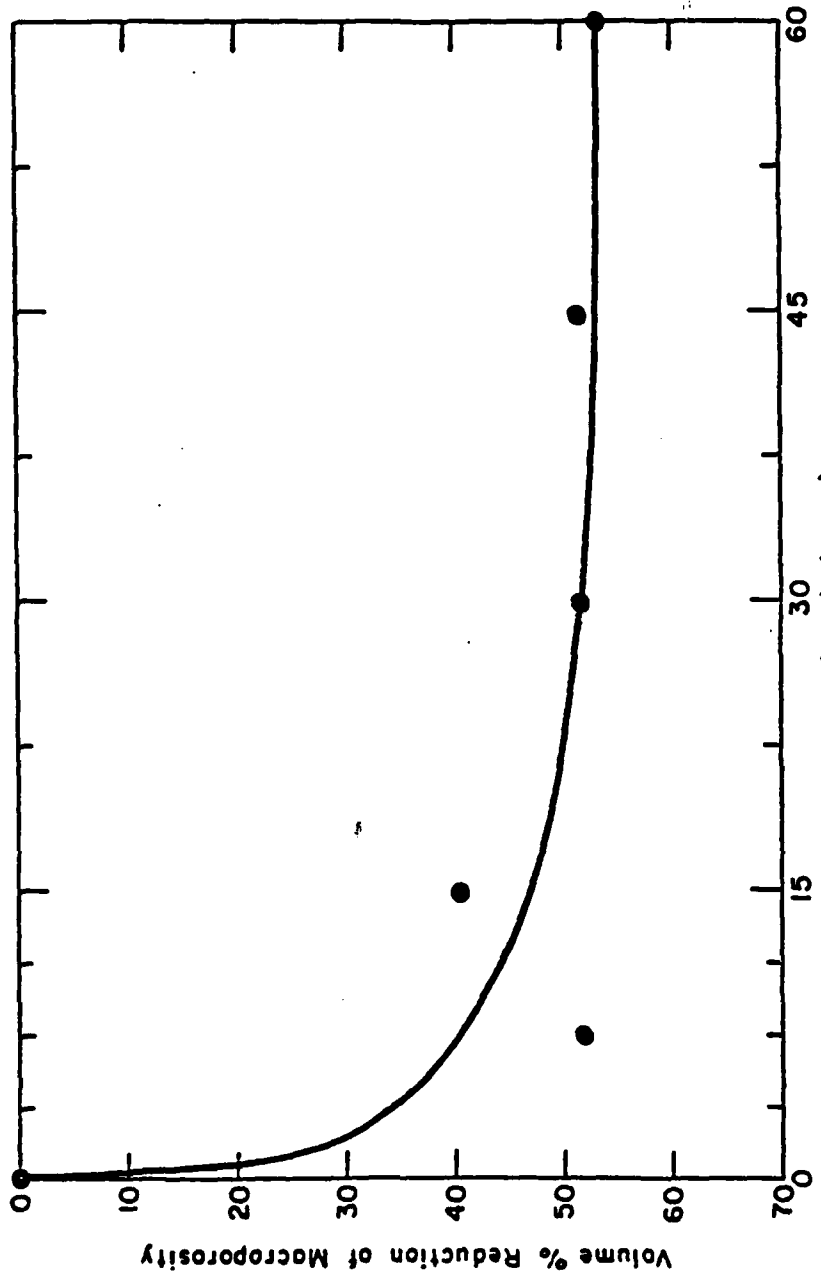

Figure 13. The volume percent reduction of macroporosity as a function of HIP time at 1300°C and 6.9 MPa.

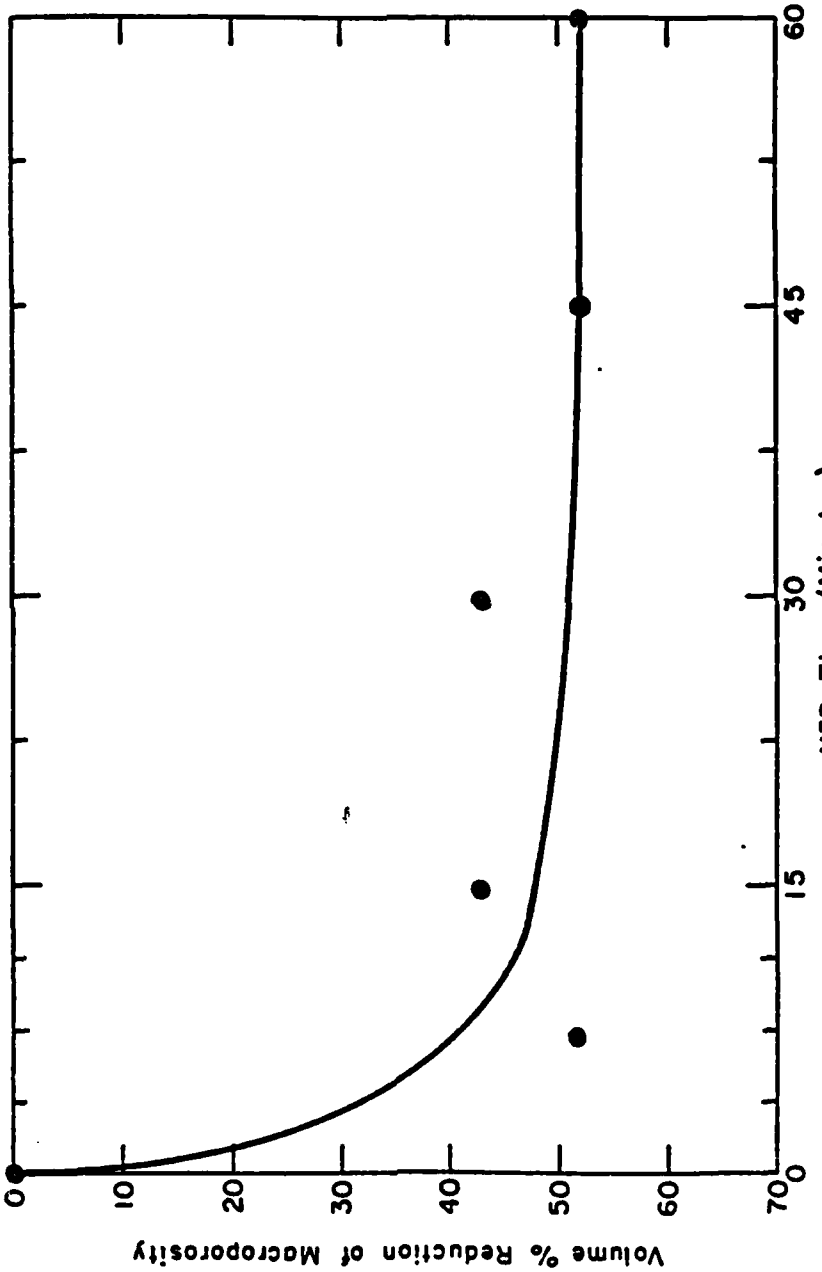

Figure 14. The volume percent reduction of macroporosity as a function of HIP time at 1300°C and 13.8 MPa.

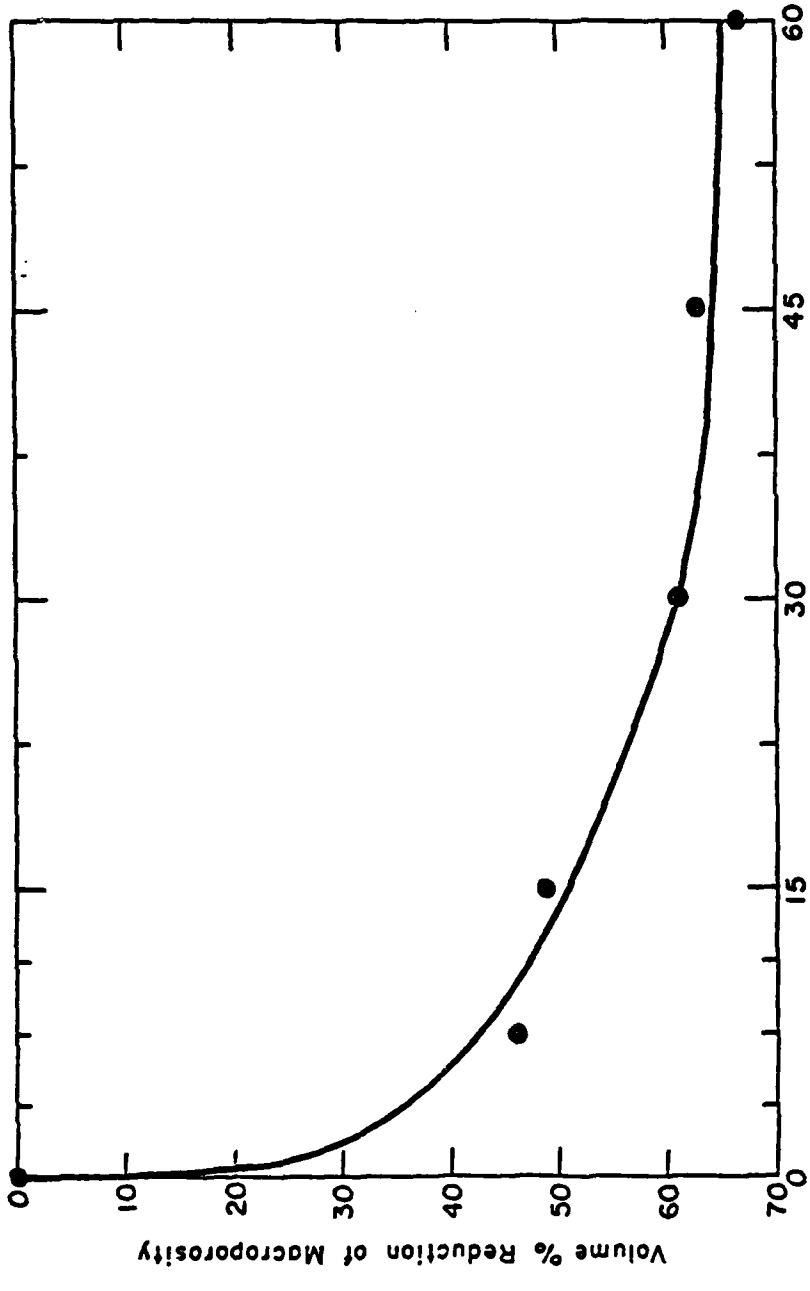

Figure 15. The volume percent reduction of macroporosity as a function of HIP time at 1300°C and 20.7 MPa.

microporosity is defined here as any porosity that occurs in the sample that is not attributable to the addition of the polymethyl methacrylate spheres. Since it is beyond the scope of this thesis to study microporosity directly (e.g., TEM), the information available was used to calculate the total amount of microporosity present in samples. The total volume percent of porosity ($\%V_{total}$) can be determined from the density measurements. Knowing the total volume percent of macroporosity originally present in the sintered body (1.21%) and the change in the volume of macroporosity as a function of HIP time, the volume percent of macroporosity can be determined from the equation:

$$\%V_{macro} = 1.21\% \ (1-\Delta V_{macro})$$

The volume percent of microporosity ($\%V_{micro}$) can then be determined from the difference of these:

$$\%V_{micro} = \%V_{total} - \%V_{macro}$$

Tables 6-8 show the changes in total, macro-, and microporosity levels as a function of HIP time at the various pressing pressures. In Figures 16-18, it is observed that the amounts of total and macroporosity decrease rapidly in the first 15 minutes, and remain constant at longer times. Unexpectedly, though, a rapid increase in the amount of microporosity is observed for the first 15 minutes. This could be the result of either the development of new pores or the growth of existing micropores. However, it is not obvious how micropores would grow, as current theories predict their shrinkage. Therefore, it is believed that new pores are being formed during HIPing. A similar phenomenon has been observed in compressive

Table 6

The Change in Total, Macro-, and Microporosity Levels as a Function of HIP Time at 1300°C and 6.9 MPa

HIP Time (min)	Volume % Porosity		
	Total	Macro	Micro
0.0	2.68	1.21	1.46
7.5	2.52	0.57	1.95
15.0	2.41	0.71	1.70
30.0	2.36	0.57	1.79
45.0	2.27	0.57	1.70
60.0	2.38	0.56	1.82

Table 7

The Change in Total, Macro-, and Microporosity Levels as a Function of HIP Time at 1300°C and 13.8 MPa

HIP Time (min)	Volume % Porosity		
	Total	Macro	Micro
0.0	2.68	1.21	1.47
7.5	2.41	0.57	1.84
15.0	2.35	0.69	1.66
30.0	2.29	0.69	1.60
45.0	2.36	0.57	1.79
60.0	2.44	0.57	1.87

Table 8

The Change in Total, Macro-, and Microporosity Levels as a Function of HIP Time at 1300°C and 20.7 MPa

HIP Time (min)	Volume % Porosity		
	Total	Macro	Micro
0.0	2.68	1.21	1.47
7.5	1.95	0.65	1.30
15.0	2.34	0.61	1.73
30.0	2.37	0.47	1.90
45.0	2.26	0.44	1.82
60.0	2.08	0.40	1.68

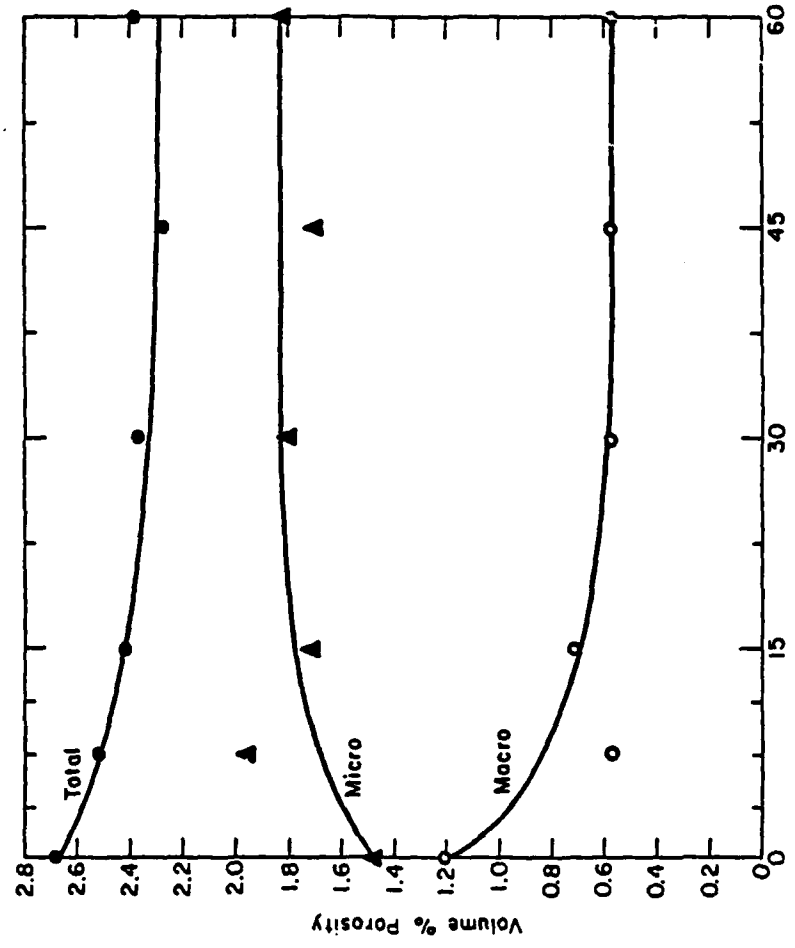

Figure 16. The change in total, macro-, and microporosity levels as a function of HIP time at 1300°C and 6.9 MPa.

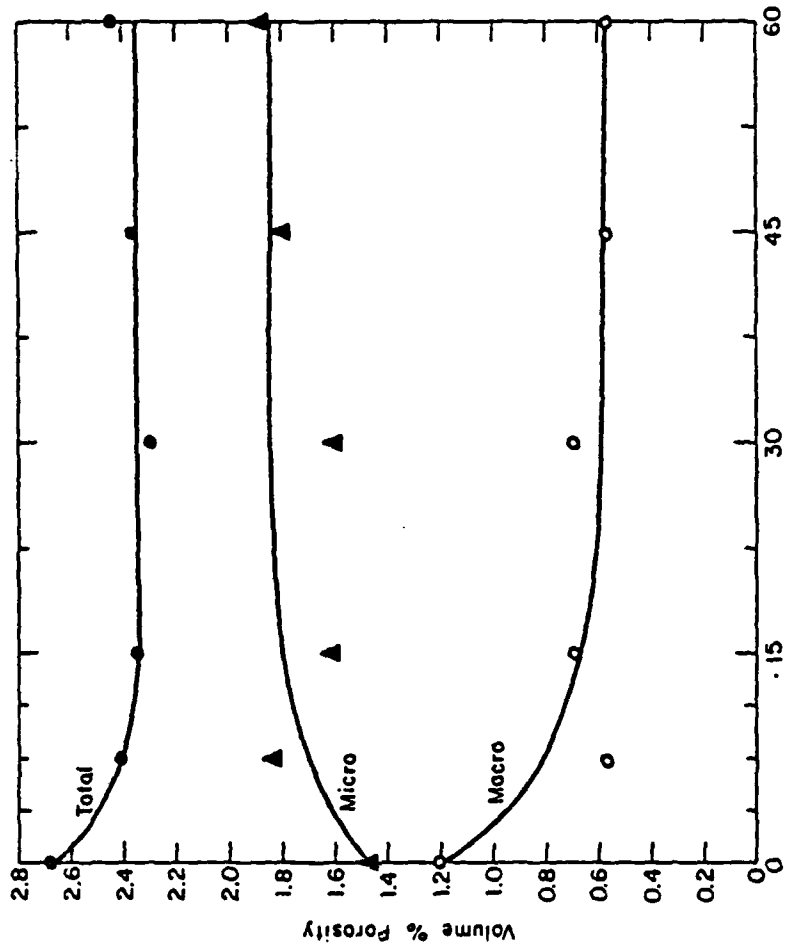

Figure 17. The change in total, macro-, and microporosity levels as a function of HIP time at 1300°C and 13.8 MPa.

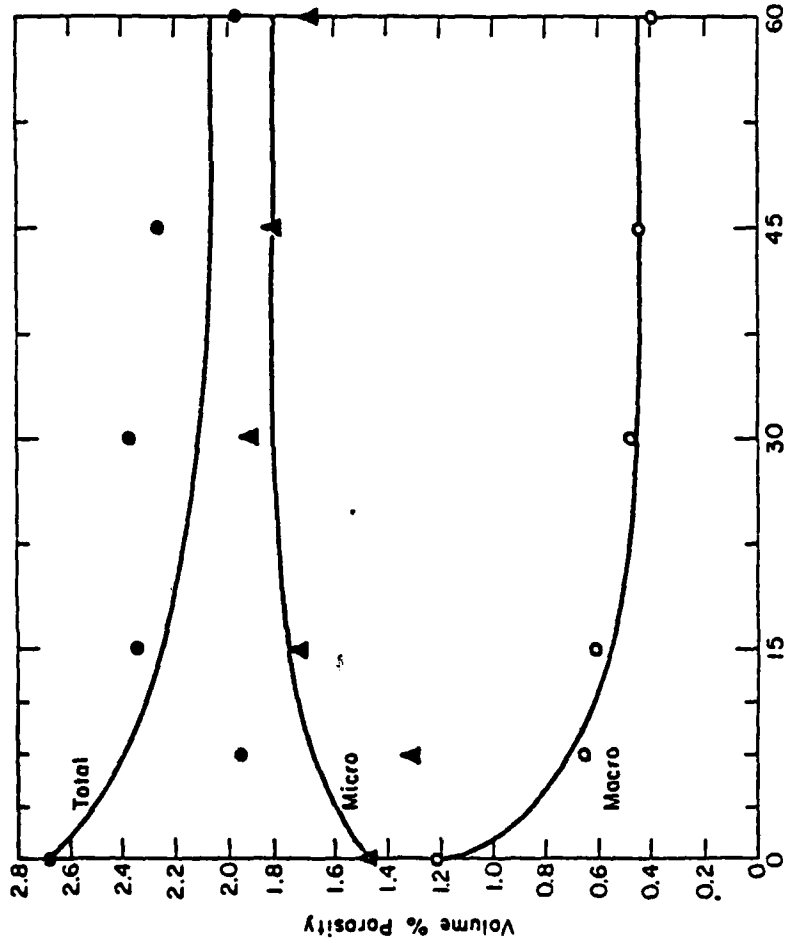

Figure 18. The change in total, macro-, and microporosity levels as a function of HIP time at 1300°C and 20.7 MPa.

creep experiments,[50] and is known as cavitation. It is believed that, during HIPing, cavities are created about macropores due to the rearrangement of grains in that region. Evidence of this can be seen in Figure 19.

Microstructure. The microstructure in and about macropores in HIPed PZT (Figure 19) is quite different from that previously observed in the sintered PZT. After HIPing, the deformation of macropores during densification is evidenced by the rough pore surfaces. Also, it appears that localized microstructural inhomogeneities result from HIPing. Tetragonal crystals are observed on the pore surface, and a "dense phase" is present on the pore periphery. The presence of tetragonal crystals is consistent with what would be expected based on the phase diagram (Figure 4). The dense phase present is compositionally analogous to the liquid phase observed at triple points in HIPed PZT. This lends additional support to the hypothesis that liquid is being squeezed into porous regions during HIPing.

Microprobe analysis (Table 9) of the microstructural variations in and about macropores indicates that both the dense phase and the crystals are $PbTiO_3$-rich PZT. The bulk of the material has a $PbZrO_3$:$PbTiO_3$ molar ratio of ~53:47 while the dense phase on the periphery and the crystalline phase on the macropore surface have molar ratios of ~40:60 and ~10:90, respectively. These results indicate that the composition of the PZT becomes increasingly rich in $PbTiO_3$ as one goes from the matrix to the center of the pore.

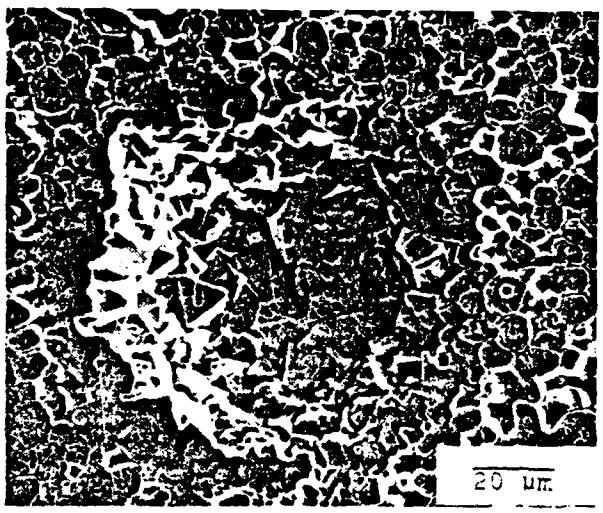

Figure 19. Photomicrograph of the sintered PZT after HIPing for 45 minutes at 1300°C and 13.8 MPa. Note the crystals formed in the macropore and the dense region surrounding the pore.

Table 9

Microprobe Analysis of the Microstructural Inhomogeneities In and About Macropores in PZT HIPed for 1 Hour at 1300°C and 20.7 MPa

	Bulk	Crystal	Dense Phase
PbO (wt %)	58.74	63.35	60.69
SrO (wt %)	1.44	0.77	1.25
ZrO_2 (wt %)	24.57	5.80	18.74
TiO_2 (wt %)	15.25	30.08	19.32

This can be explained by considering isothermal sections of the $PbO-PbZrO_3-PbTiO_3$ ternary phase diagram (Figure 20).

Initially, a solid of composition S_1 and a liquid of composition L_1 are present at the HIPing temperature of 1300°C (Figure 20a). The slight excess of PbO present in the system is responsible for the liquid phase observed, and it is the nonequilibrium cooling of this liquid that produces the compositional variations observed. As the system is cooled, the changing equilibrium between the liquid and solid will result in the solidification of PZT that is increasingly richer in $PbTiO_3$ (Figures 20b and 20c). The results presented earlier are consistent with this, as the PZT at the macropore surface would be expected to have the highest concentration of $PbTiO_3$.

The microstructural variations observed are not as easily explained. The migration of liquid to the pores can account for the microstructure on the pore periphery, but does not explain why

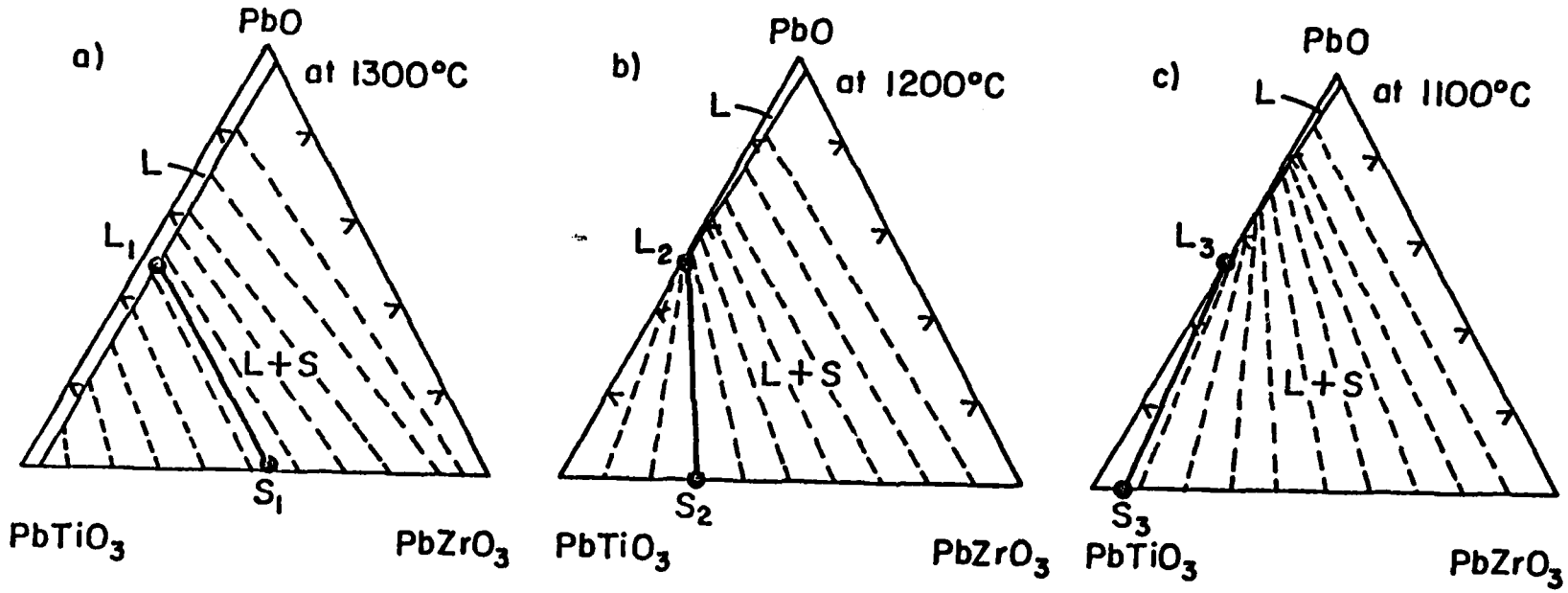

Figure 20. Isotherms of the system PbO-$PbZrO_3$-$PbTiO_3$ at 1300°, 1200°, and 1100°C.[61]

crystals are formed at the pore surface. It is suggested that pressure is at least partially responsible since heat treating HIPed samples for 10 hours at 1320°C (atmospheric pressure) results in the disappearance of these crystals (Figure 21). Further work would be required to determine exactly why these crystals are formed during HIPing.

Mechanisms. The results obtained from the HIP experiments give an indication of the mechanisms by which the macropores shrink during HIPing. The rapid increase in density and decrease in macroporosity in short HIP times suggest that kinetics are initially controlled by a rearrangement and/or solution-precipitation process. Arguments for a rearrangement process are supported by the presence of a liquid phase in and about macropores, and grain rearrangement on macropore surfaces (Figure 22). There is no direct evidence for a solution-precipitation process, but the presence of a liquid phase with a high solubility for the solid PZT suggests that it must be occurring. From the information available, it is impossible to determine exactly how much of each contributes to the initial densification; however, both are believed to play important roles.

End point densities less than the theoretical density of the PZT suggest that a slow process (i.e., diffusion) ultimately controls densification. Internal pressures resulting from the compression of gases trapped within pores during sintering do not appear to be responsible for the end point densities. This is argued on the basis that oxygen would be the gas entrapped in the pores. Thus, it would have readily diffused through the PZT lattice to relieve any pressure buildup resulting from pore shrinkage. Likewise,

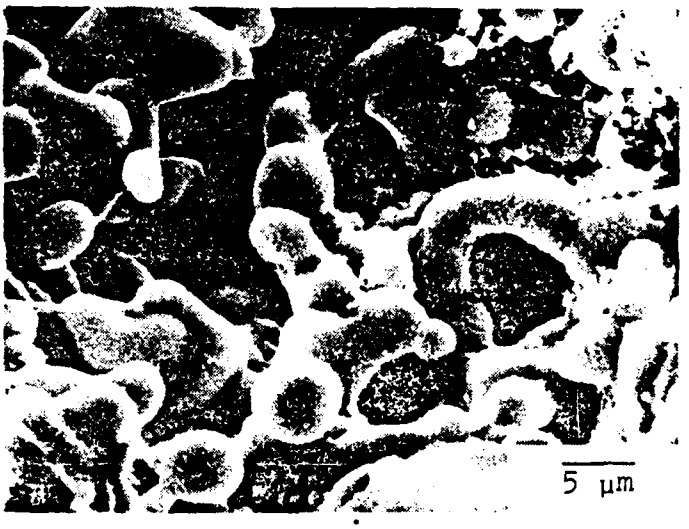

Figure 21. Photomicrograph of a macropore in a sample that has been heat treated for 10 hours at 1320°C after HIPing.

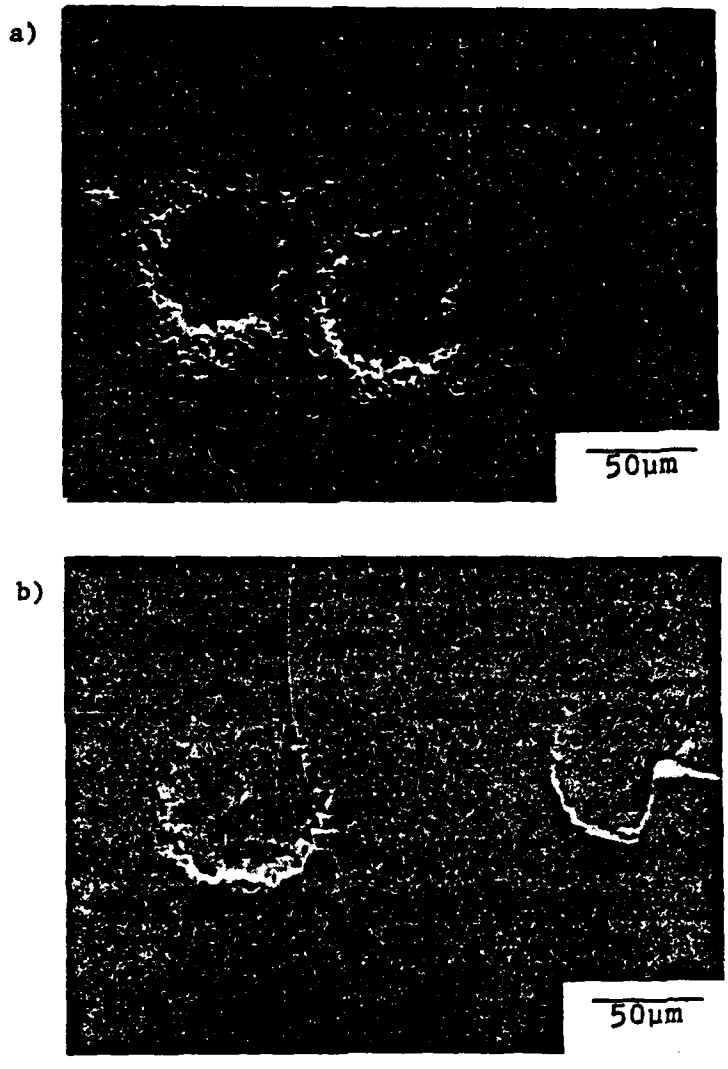

Figure 22. Photomicrograph indicating grain rearrangement at macropore surfaces in PZT samples HIPed for 7.5 minutes at 1300°C and a) 13.8 MPa and b) 20.7 MPa.

growth of micropores due to entrapped oxygen can also be discounted as the gas would have been trapped at the sintering temperature (1320°C), and therefore could not have expanded at the lower HIPing temperature (1300°C). These results indicate that ~98% represents the end point density for the conditions studied.

Electrical Properties

The electrical property measurements of samples sintered with and without macropores are presented in Table 10. Only one sample was obtained from a given pellet for electrical measurements, and this was always taken from the interior of the pellet. It was assumed that the electrical properties of the sample would be representative of both the pellet and the processing conditions. Many samples were lost due to dielectric breakdown during poling, and this accounts for the small and variable number of samples measured. It is suggested that the major reason for the high losses during poling was the large size of macroporosity (~100 micrometers) with respect to sample thickness (~600 micrometers). A higher probability of failure exists for small samples containing defects than for large ones. Also, the larger the defect, the more deletereous the effect on dielectric breakdown strength.[21] This is the case in this study as the relatively large pores in the small samples substantially reduced dielectric breakdown strength. Approximately 50% of the samples containing macropores broke down during poling while only 10% of those without macropores failed. Also, the effect of size was evident as HIPed samples containing

Table 10

Room Temperature Electrical Properties of PZT Samples Sintered for 1 Hour at 1320°C With and Without Macropores

Sample	With Macropores				Without Macropores		
	1	2	3	Average	1	2	Average
Dielectric Constant at 1000 Hz	1335	1290	1305	1310	1425	1410	1415
Dissipation Factor at 1000 Hz	0.008	0.009	0.005	0.007	0.003	0.004	0.004
Piezoelectric Coefficient, d_{33}, at 100 Hz ($C/N \times 10^{-12}$)	310	290	310	300	300	310	305
Radial Coupling Coefficient (%)	51	52	52	52	54	56	55
Young's Modulus, Y_{11} ($N/m^2 \times 10^{11}$)	1.6	1.6	1.7	1.6	1.7	1.6	1.7
Radial Frequency Constant (m · Hz)	2340	2340	2350	2340	2340	2325	2335

pores slightly smaller than those present in sintered samples showed a slightly lower probability of failure (~40%). Overall, these results are in agreement with observations made by Gerson and Marshall.[21]

Since electrical measurements were made on only a limited number of samples, the statistical accuracy is not as good as desired. However, general trends can still be observed. Both dielectric constant and radial coupling coefficient are apparently higher in sintered samples without the macropore addition. Also, dielectric losses are lower in these samples. This indicates that the macropore addition does in fact adversely affect electrical properties. This is in agreement with the findings of Okazaki and Nagata,[62] who showed that, in PZT, electrical properties are adversely affected with increasing levels of porosity.

Electrical properties of HIPed samples (with macropores) are shown in Tables 11-13. Since the physical properties obtained by HIPing at all three pressing pressures are similar, it is expected that the resultant electrical properties should also be similar. Therefore, electrical measurements were made only on samples HIPed at 20.7 MPa. Samples HIPed for 7.5, 15, and 60 minutes were measured to determine whether or not a correlation exists between the electrical properties and density. As shown in Table 14, there is no clear trend. This is probably due to the fact that only small changes in density resulted from HIPing. However, it is believed that a positive trend (i.e., improved properties) would have been observed had higher densities (e.g., ~theoretical) been obtained. Electrical properties were also determined for samples

Table 11

Room Temperature Electrical Properties of PZT With Macropores HIPed for 7.5 Minutes at 1300°C and 20.7 MPa

Sample	1	2	Average
Dielectric Constant at 1000 Hz	1355	1350	1355
Dissipation Factor at 1000 Hz	0.006	0.009	0.008
Piezoelectric Coefficient, d_{33}, at 100 Hz ($C/N \times 10^{-12}$)	320	320	320
Radial Coupling Coefficient (%)	56	54	55
Young's Modulus, Y_{11} ($N/m^2 \times 10^{11}$)	1.7	1.8	1.8
Radial Frequency Constant (m · Hz)	2335	2365	2350

Table 12

Room Temperature Electrical Properties of PZT With Macropores HIPed for 15 Minutes at 1300°C and 20.7 MPa

Sample	1	2	3	4	Average
Dielectric Constant at 1000 Hz	1360	1300	1235	1255	1290
Dissipation Factor at 1000 Hz	0.007	0.010	0.014	0.015	0.012
Piezoelectric Coefficient, d_{33}, at 100 Hz ($C/N \times 10^{-12}$)	310	300	270	280	290
Radial Coupling Coefficient (%)	53	51	50	50	51
Young's Modulus, Y_{11} ($N/m^2 \times 10^{11}$)	1.7	1.8	1.7	1.6	1.7
Radial Frequency Constant (m · Hz)	2355	2380	2345	2330	2350

Table 13

Room Temperature Electrical Properties of PZT With Macropores HIPed for 1 Hour at 1300°C and 20.7 MPa

Sample	1	2	Average
Dielectric Constant at 1000 Hz	1390	1380	1385
Dissipation Factor at 1000 Hz	0.006	0.010	0.008
Piezoelectric Coefficient, d_{33}, at 100 Hz ($C/N \times 10^{-12}$)	300	300	300
Radial Coupling Coefficient (%)	53	51	52
Young's Modulus, Y_{11} ($N/m^2 \times 10^{11}$)	1.7	1.7	1.7
Radial Frequency Constant (m · Hz)	2555	2580	2565

Table 14

Room Temperature Electrical Properties of PZT With Macropores as a Function of HIP Time at 1300°C and 20.7 MPa

HIP Time (minutes)	0*	7.5	15	60
Dielectric Constant at 1000 Hz	1310	1355	1290	1385
Dissipation Factor at 1000 Hz	0.007	0.008	0.012	0.008
Piezoelectric Coefficient, d_{33}, at 100 Hz ($C/N \times 10^{-12}$)	300	320	290	300
Radial Coupling Coefficient (%)	52	55	51	52
Young's Modulus, Y_{11} ($N/m^2 \times 10^{11}$)	1.6	1.8	1.7	1.7
Radial Frequency Constant (m · Hz)	2340	2350	2350	2565

* Sintered

HIPed without macropores (Table 15). Again, no relationship between electrical properties and density is observed. This result indicates that, for the conditions studied, HIPing has no effect on the electrical properties of sintered PZT.

Table 15

Room Temperature Electrical Properties of PZT Without Macropores as a Function of HIP Time at 1300°C and 20.7 MPa

HIP Time (minutes)	0*	7.5	15	60
Dielectric Constant at 1000 Hz	1415	1250	1310	1250
Dissipation Factor at 1000 Hz	0.005	0.007	0.006	0.006
Piezoelectric Coefficient, d_{33}, at 100 Hz ($C/N \times 10^{-12}$)	305	290	290	290
Radial Coupling Coefficient (%)	55	47	48	52
Young's Modulus, Y_{11} ($N/m^2 \times 10^{11}$)	1.7	1.6	1.5	1.6
Radial Frequency Constant (m · Hz)	2335	2320	2300	2340

* Sintered

SUMMARY AND CONCLUSIONS

The effects of hot isostatic pressing sintered lead zirconate titanate with low pressures (6.9 - 20.7 MPa) were studied. Gross composition and grain size were unaffected. Slight increases in density were observed for all conditions studied, with the kinetics of densification indicating a two-stage process. Macroporosity was substantially reduced in size and volume percent while the amount of microporosity increased. Compositional and microstructural variations in and about macropores indicated the migration of $PbTiO_3$-rich liquid to the pores. Rapid kinetics, microstructural analysis, and the presence of a liquid phase about macropores suggest that rearrangement and solution-precipitation may be responsible for initial densification. End point densities of approximately 98% indicate that a solid state diffusion process ultimately controls densification.

A substantial decrease in dielectric breakdown strength was observed in lead zirconate titanate samples containing large voids. Hot isostatic pressing to reduce the size of these voids improved the breakdown strength. The unclamped dielectric constant, dissipation factor, piezoelectric coefficient d_{33}, radial coupling coefficient, radial frequency constant, and Young's modulus of sintered lead zirconate titanate were unaffected by hot isostatic pressing.

REFERENCES

1. Jaffe, B., Cook, W.R., Jr., and Jaffe, H., Piezoelectric Ceramics. New York, New York: Academic Press, Inc., (1971).

2. Kingon, A.I., "Studies in the Preparation and Characterization of Selected Ferroelectric Materials," Ph.D. Thesis, University of S. Africa, (1981).

3. Kulcsar, F., "Electromechanical Properties of Lead Titanate Zirconate Ceramics Modified with Certain Three or Five-Valent Additions," J. Am. Ceram. Soc., 42 [7], 343-49, (1959).

4. Gerson, R., "Variations in Ferroelectric Characteristics of Lead Zirconate Titanate Ceramics Due to Minor Chemical Modifications," J. Appl. Phys., 31 [1], 188-94, (1960).

5. Weston, T.B., Webster, A.H., and McNamara, V.M., "Lead Zirconate-Lead Titanate Ceramics with Iron Oxide Additions," J. Am. Ceram. Soc., 52 [5], 253-57, (1969).

6. Banno, H. and Tsunooka, T., "Piezoelectric Properties and Temperature Dependencies of Resonant Frequency of WO_3 - MnO_2 - Modified Ceramics of $Pb(Zr-Ti)O_3$," Jap. J. Appl. Phys., 6 [8], 954-62, (1967).

7. Kulcsar, F., "Electromechanical Properties of Lead Titanate Zirconate Ceramics with Lead Partially Replaced by Calcium or Strontium," J. Am. Ceram. Soc., 42 [1], 49-51, (1959).

8. Ikeda, T. and Okano, T., "Piezoelectric Ceramics of $Pb(Zr-Ti)O_3$ Modified by $A^{1+}B^{5+}O_3$ or $A^{3+}B^{3+}O_3$," Jap. J. Appl. Phys., 3 [2], 63-71, 1964).

9. Lee, D.C., "Sintering Sc and Nb Modified Lead Zirconate Titanate," M.S. Thesis, University of California, Berkeley, (1972), LBL-880.

10. Atkin, R.B., "Sintering and Ferroelectric Properties of Lead Zirconate Titanate Ceramics," D. Eng. Thesis, University of California, Berkeley, (1970), UCRL-20309.

11. Levett, P.D., "Factors Affecting Lead Zirconate-Lead Titanate Ceramics," Am. Ceram. Soc. Bull., 42 [6], 348-52, (1963).

12. Webster, A.H., Weston, T.B., and Bricht, N.F.H., "Effect of PbO Deficiency on the Piezoelectric Properties of Lead Zirconate Titanate Ceramics," J. Am. Ceram. Soc., 50 [9], 490-91, (1967).

13. Chaing, S., Nishoika, M., Fulrath, R.M., and Pask, J.A., "Effect of Processing on Microstructure and Properties of PZT Ceramics," Am. Ceram. Soc. Bull., 60 [4], 484-89, (1981).

14. Haertling, G., "Hot-Pressed Lead Zirconate-Lead Titanate Ceramics Containing Bismuth," Am. Ceram. Soc. Bull., 43 [12], 875-79, (1964).

15. Webster, A.H., "The Effects of Some Fabrication Conditions on the Properties of Lead Zirconate-Lead Titanate Ceramics," Canada Department of Mines and Tech. Surveys, Mines Branch Investigation Report IR 63-59, July, 1963.

16. Webster, A.H., Weston, T.B., and McNamara, V.M., "The Effects of Some Variations in Fabrication Procedure on the Properties of Lead Zirconate-Titanate Ceramics Made From Spray-Dried Co-Precipitated Powders," J. Can. Ceram. Soc., 35, 61-68, (1966).

17. Webster, A.H., Weston, T.B., and Craig, R.R., "Some Ceramic and Electrical Properties of Bodies Fabricated from Co-Precipitated Lead-Zirconium-Titanium Hydroxide," J. Can. Ceram. Soc., 34, 121-129, (1965).

18. Multani, M.S., Gokarn, S.G., Vijayaraghavan, R., and Palkar, V.R., "Morphotropic Phase Boundary in the $Pb(Zr_xTi_{1-x})O_3$ System," PIG-13, Abstracts, Fifth International Meeting on Ferroelectricity, August 17-21, 1981.

19. Klicker, K.A., "Control of PbO Partial Pressure During the Sintering of PZT Ceramics," M.S. Thesis, The Pennsylvania State University, (1979).

20. Hankey, D.L., "Calcination Reaction Mechanisms and Kinetics in $PbO-TiO_2-ZrO_2$ Powder Compacts," Ph.D. Thesis, The Pennsylvania State University, (1980).

21. Gerson, R. and Marshall, T.C., "Dielectric Breakdown of Porous Ceramics," J. Appl. Phys., 30 [11], 1650-53, (1959).

22. Biswas, D.R., "Electrical Properties of Porous PZT Ceramics," J. Am. Ceram. Soc., 61 [9-10], 461-2, (1978).

23. Webster, A.H. and Weston, T.B., "The Grain-Size Dependence of the Electromechanical Properties in Lead Zirconate-Titanate Ceramics," J. Can. Ceram. Soc., 37, XLI-XLIV, (1968).

24. Atkin, R.B. and Fulrath, R.M., "Point Defects and Sintering of Lead Zirconate-Titanate," J. Am. Ceram. Soc., 54 [5], 265-70, (1971).

25. Sherohman, J.W., Jr., "A Liquid Phase Densification Technique for the Lead Zirconate Titanate System," Ph.D. Thesis, University of California, Berkeley, (1974), LBL-2767.

26. Bowen, L.J., Shrout, T.R., Venkataramani, S., and Biggers, J.V., "Inhomogeneous Densification During Sintering of PZT," In print.

27. Crabtree, K.E., "Densification and Electrical Properties of Controlled Stoichoimetry PZT," M.S. Thesis, University of California, Berkeley, (1974), LBL-3543.

28. Semans, B.F., "Densification and Electrical Properties of Lead Zirconate Titanate," M.S. Thesis, University of California, Berkeley, (1968), UCRL-18126.

29. Hall, C.E. and Blum, J.B., "Effect of Sintering Heating Rate on the Electrical Properties of Sr-PZT," Ferroelectrics, 37, 643-46, (1981).

30. Venkataramani, S. and Biggers, J.V., "Densification in PZT," Ferroelectrics, 37, 607-10, (1981).

31. Kim, Y.S. and Hart, R.J., "Processing of High Density Piezoelectric Ceramic Compositions," in Processing of Crystalline Ceramics, Materials Science Research, Vol. 11, Palmour, H., III, Davis, R.F., and Hare, T.M. (eds.). New York: Plenum Press, 323-33, (1978).

32. Murray, T.F. and Dungan, R.H., "Oxygen Firing Can Replace Hot Pressing for PZT," Ceram. Ind., 82-83 [7], 74-77, (1964).

33. Sahm, P.R., "Powder Metallurgical Review 2. Pressure Sintering - A Versatile Method of Materials' Preparation (Part I)," Powder Met., 3 [1], 45-49, (1971).

34. Sahm, P.R., "Powder Metallurgical Review 2. Pressure Sintering - A Versatile Method of Materials' Preparation (Part II)," Powder Met., 3 [2], 95-100, (1971).

35. Chaklader, A.C.D., "Theories of Hot Pressing," J. Can. Ceram. Soc., 40, 19-28, (1971).

36. Coble, R.L., "Diffusion Models for Hot Pressing with Surface Energy and Pressure Effects as Driving Forces," J. Appl. Phys., 41 [12], 4798-4807, (1970).

37. Spriggs, R.M., "Hot Pressed Oxides," in High Temperature Oxides, Part III, Alper, A.M. (ed.), New York: Academic Press, 183-234, (1970).

38. Mountvala, A.J., "Hot Pressing Piezoelectric and Ferroelectric Materials," Am. Ceram. Soc. Bull., 42 [3], 120-21, (1963).

39. Balkevich, V.L. and Flidlider, C.M., "Hot Pressing of Some Piezoelectric Ceramics in the PZT System," Ceram. Int., 2 [2], 81-87, (1976).

40. Haertling, G.H. and Zimmer, W.J., "An Analysis of Hot-Pressing Parameters for Lead Zirconate Titanate Ceramics Containing Two Atom Percent Bismuth," Am. Ceram. Soc. Bull, 45 [12], 1084-89, (1966).

41. Okazaki, K., "Sintering Processes of Lead Zirconate-Lead Titanate Ceramics by Hot Pressing and Their Electrical Properties," Memoirs of the Defense Academy of Japan, VII, [2], 383-98, (1967).

42. Coble, R.L., "Hot Consolidation of Rapidly Solidified Powders: Sintering, Hot Pressing (HP), and Hot Isostatic Pressing (HIP) in Relation to the Superalloys," Powder Met. Int., 10 [3], 128-30, (1978).

43. Fischmeister, H., "Isostatic Hot Compaction - A Review," Powder Met. Int., 10 [3], 119-22, (1978).

44. Traff, A. and Skotte, P., "Isostatic Pressing of Ceramic Materials, Methods and Trends," Powder Met. Int., 8 [2], 65-68, (1976).

45. James, P.J., "Hot Isostatic Pressing: An Economic Route to Powder Components," Metals and Materials, 11 [11], 27-31, (1977).

46. Porembka, S.W., "Gas Pressure Bonding," Ceramic Age, 79 [11], 68-71, (1963).

47. Hodge, E.S., Elevated-Temperature Compaction of Metals and Ceramics by Gas Pressures," Powder Met., 7 [14], 168-201, (1964).

48. Hanes, H.D., Seifert, D.A., and Watts, C.R., "Hot Isostatic Pressing," MCIC Report 77-34, Battelle's Columbus Laboratories, Columbus, OH, (1977).

49. Bowen, L.J., Schulze, W.A., and Biggers, J.V., "Hot Isostatic Pressing of PZT Materials," Powder Met. Int., 12 [2], 92-95, (1980).

50. Hardtl, K.H., "Gas Isostatic Hot Pressing Without Molds." Am. Ceram. Soc. Bull., 54 [2], 201-207, (1975).

51. Hardtl, K.H., "A Simplified Method for the Isostatic Hot Pressing of Ceramics," Phillips Tech. Rev., 35 [2-3], 65-72, (1975).

52. Koizumi, M., Kodaira, K., Ishitobi, M., and Kanamura, F., "Fabrication of Translucent Ceramics by Isostatic Hot-Pressing," Ceram. Int., 2 [2], 67-71, (1976).

53. Ishitobi, Y., Shimada, M., and Koizumi, M., "Fabrication of Translucent $Pb(Zr_{0.8}Ti_{0.2})O_3$ Ceramics by Isostatic Hot Pressing," J. Am. Ceram. Soc., 57 [10], 458, (1974).

54. Ewsuk, K.G. and Messing, G.L., "Isostatic Hot Pressing of Sintered Lead Zirconate Titanate," Ceram. Engr. and Sci. Proc., 2 [7-8], 450-55, (1981).

55. Fullman, R.L., "Measurement of Particle Sizes in Opaque Bodies," Trans AIME, 197 [3], 447-52, (1953).

56. "IRE Standards on Piezoelectric Crystals: Determination of the Elastic, Piezoelectric, and Dielectric Constants - the Electromechanical Coupling Factor, 1958," Proc. IRE, 46, 764-78, (1958).

57. Kingery, W.D. and Francois, B., "The Sintering of Crystalline Oxides, I. Interactions Between Grain Boundaries and Pores," in Sintering and Related Phenomena, Kuczynski, G.C., Hooton, N.A., and Gibbon, C.F. (eds.). New York: Gordon and Breach Science Publishers, Inc., 471-98, (1967).

58. Goo, E.K.W., Mishra, R.K., and Thomas, G., "Transmission Electron Microscopy of $Pb(Zr_{0.52}Ti_{0.48})O_3$," J. Am. Ceram. Soc., 64, [9], 517-519, (1981).

59. Lang, F.F., "Liquid Phase Sintering: Are Liquids Squeezed Out From Between Compressed Particles?" Communications of the Am. Ceram. Soc., [2], C-23, (1982).

60. Lange, F.F., Davis, B.I., and Clarke, D.R., "Compressive Creep of Si_3N_4/MgO Alloys," J. Mat. Sci., 15, 601-610, (1980).

61. Fushimi, S. and Ikeda, T., "Phase Equilibrium in the System $PbO-TiO_2-ZrO_2$," J. Am. Ceram. Soc., 50, [3], 129-132, (1967).

62. Okazaki, K. and Nagata, K., "Effects of Density and Grain Size on the Elastic and Piezoelectric Properties of $Pb(Zr-Ti)O_3$ Ceramics," Proc. 1971 Int'l. Conf. on Mechanical Behavior of Materials, Vol. 4, 404-512.

DISTRIBUTION LIST FOR TM 82-238

Commander (NSEA 0342)
Naval Sea Systems Command
Department of the Navy
Washington, DC 20362

Copies 1 and 2

Commander (NSEA 9961)
Naval Sea Systems Command
Department of the Navy
Washington, DC 20362

Copies 3 and 4

Defense Technical Information Center
5010 Duke Street
Cameron Station
Alexandria, VA 22314

Copies 5 through 10

END

FILMED

2-83

DTIC